SPATIO-TEMPORAL TRACKING OF MELANOCYTIC DIFFERENTIATION AND MIGRATION OF CRANIAL NEURAL CREST IN ZEBRAFISH EMBRYONIC DEVELOPMENT

A Thesis

by

BENJAMIN PATRICK ROBERTSON

Submitted to the Office of Graduate and Professional Studies of
Texas A&M University
in partial fulfillment of the requirements for the degree of

MASTER OF SCIENCE

Chair of Committee,	Alvin Yeh
Committee Members,	Arne Lekven
	Kristen Maitland
Head of Department,	Anthony Guiseppi-Elie

August 2016

Major Subject: Biomedical Engineering

ABSTRACT

We set out to characterize a population of midbrain fluorescing cells in zebrafish that appeared to be of melanophore lineage and in doing so discovered a potential role for *sox10* expression in the zebrafish central nervous system glial cell network. A decrease in the signal of interest correlated with increased inhibition of melanin production by PTU (1-phenyl-2-thioreau) treatment; however, the autofluorescence signal at question was determined not to be associated with melanin biosynthesis after wild type time lapse imaging experiments showed the absence of said signal, and it was shown that only after fixation of the embryos was the signal produced. To characterize these strongly autofluorescing cells, melanophore gene expression was visualized using transgenic reporters for the transcriptions factors *sox10* and *mitfa*, a neural crest marker and a melanocyte identity regulator, respectively, via broadband ultrashort pulse excitation centered at 800 nm with FWHM of 133 nm to determine the genetic identity of the autofluorescence source via colocalization of signals. Time lapse imaging was performed to collect 4-D data sets of fluorescence reporting of the neural crest marker *sox10* and melanophore identity regulator *mitfa* within the zebrafish midbrain between the prim-5 and prim-25 stage, revealing a novel population of *sox10* expressing cells within the neuroepithelium that proliferates and migrates within the ventral midbrain tissue towards the developing nasal cavity, suggesting a role *sox10* may play in oligodendrocyte regulatory networks in this region. Gene expression visualization of *mitfa* in the same region displayed no neuroepithelial expression as expected.

DEDICATION

The work presented in this thesis is dedicated to my loving and supportive parents Charles and Julie Robertson, who have helped me in every step of the way in my scholastic pursuits and who always believed in me even when I did not believe in myself. The hours of work that will not be presented but that were wholly necessary are dedicated to my grandfather, Lawrence Gentry, who taught me that hard work and perseverance are the truest measures of a man. All the time I would have rather spent fishing with my grandmother, Sarah Gentry, is dedicated to her for showing us boys how to bait a hook and do the gritty things in life, like dispatch an opossum with a fireplace rod. Lastly, this effort is dedicated to my best friend Alexandra Perez Olalla. Thanks for inspiring confidence in me every day and most of all thank you for your patience, encouragement, and love.

ACKNOWLEDGEMENTS

I want to thank Dr. Alvin Yeh for his wise and friendly mentorship during my last two years at Texas A&M University. I appreciate that you took a genuine interest in my work and that you taught me to start asking the right questions. Thanks for all of the patience and advice you gave me in brainstorming sessions and also for your sense of humor through it all. I must also give a huge thank-you to Dr. Holly Gibbs. You showed me the ropes in the lab and you are the only person I can commiserate with on so many levels (dechorionating, time lapse experiments, stack adjustments). Thanks for answering my dumbest questions and helping me find answers to my toughest, I wish I could make you my fourth committee member. Speaking of committee members I also want to acknowledge Dr. Kristen Maitland and Arne Lekven for their guidance and advice. I also want to thank Dr. Arne Lekven for his extraordinary guidance in zebrafish biology and for facilitating my use of the BSBE fish rooms. His impressive knowledge of developmental biology aided me immensely. The Lekven group taught me almost everything I know about the biological protocols I used to conduct my thesis work, namely Amy Whitener, David Green, and Jo-Ann Fleming. Much gratitude is due to Amy, David, and Joann for their constant help in the zebrafish lab and the conversations we had together. Lastly I want to thank Stan Vitha of the Microscopy and Imaging Center at A&M for his generous support and kind advice.

NOMENCLATURE

SHG	Second Harmonic Generation
hpf	Hours Post Fertilization
TPEF	Two Photon Excited Fluorescence
SFG	Sum Frequency Generation
DFG	Difference Frequency Generation
WT	Wild Type
eGFP	Enhanced Green Fluorescent Protein

TABLE OF CONTENTS

Page

Page

LIST OF FIGURES

Page

Page

INTRODUCTION

The neural crest is a migratory population of cells specific to vertebrates that is a precursor to many types of cells and tissues. Often considered the fourth germ layer, the neural crest arises during the formation of the neural tube, after which these progenitor cells migrate to different destinations, each subset giving rise to components of various body systems, including but not limited to the nervous system, skeletal and connective tissues, and pigmentation (Gilbert, 2010).

Melanocytes are pigment containing cells born of the differentiating neural crest that have been shown to autofluoresce at levels much stronger (an order of magnitude greater) than normal cellular autofluorescence. A potential population of melanocytes presenting in the midbrain of zebrafish has been revealed by an intense autofluorescence signal originating at the dorsolateral hinge points of the developing neural tube (Gibbs et al.,2014). These midbrain fluorescing cells (MFCs) gain, or perhaps, retain their pigmentation while still residing within the neuro-epithelium of the neural tube wall (Figure 1), contrary to a previous understanding that melanocytes differentiate after an epithelial-to-mesenchyme transition and migration away from the neural tube (Krispin et al., 2010).

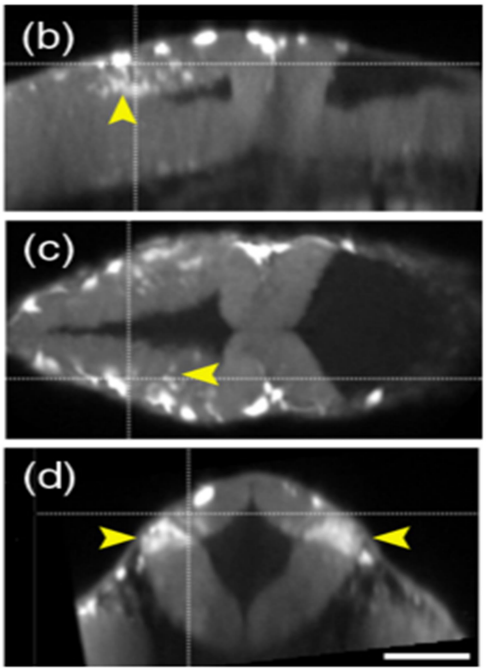

Figure 1: Midbrain fluorescing cells. Orthogonal b)lateral c)dorsal d)transverse slice views of the midbrain region revealing population of strongly fluorescing cells within neuroepithelium. Generally, cells will fluoresce upon differentiation after separation from the neuroepithelium. Yellow arrows indicate potentially differentiated populations still residing within the neural tube.

A population of melanocytes within the epithelium would suggest that differentiation occurs well before migration and disassociation from the neural tube. Knowledge of the induction, migration, and differentiation patterns of the multipotent neural crest has improved in recent years; however, a method to analyze the spatio-temporal behavior of these transient cells has yet to be developed. Fate mapping of gene reporter lines at the cellular level in space and time offers an intimate understanding of the gene regulatory networks behind several phenotypic traits in a complex organism, perhaps even mechanisms still unknown. This project aims to gain a detailed spatio-

temporal model of the induction and migration of these MFCs not previously observed, as well as define their lineage as neural crest derived melanophore or otherwise, which can be achieved through characterizing gene expression patterns in this region of interest most notably the patterns of *sox10* and *mitfa*, a neural crest lineage specifier and melanophore identity regulator, respectively.

Embryonic development at the cellular level can be observed spatio-temporally using our novel microscopy approach utilizing sub-10 femtosecond (fs) pulses to generate two photon excited cellular autofluorescence as well as fluorescent gene reporter signals, lending insight to the induction and fate of this population. It is hypothesized that this population can be identified as melanocytes or melanocytic precursor epithelial cells, furthermore identifiable as neural crest derived, provided there is a colocalized gene expression reporter signal observed where the autofluorescence signal presents for *sox10* and *mitfa*.

Motivation

It is necessary to challenge current models of the neural crest and embryonic brain development in the zebrafish so as to elucidate homologous mechanisms in humans. Orthologues of both *sox10* and *mitf* are known to be associated with Waardenburg Shah Syndrome, demyelination syndromes, and melanoma in humans, highlighting the importance of clarifying a model that potentially involves them, such as these MFCs. (Greenhill et al., 2011). The gene regulatory networks associated with the neural crest are becoming increasingly known, but the spatiotemporal activity of neural crest progenitors could be better understood; be it their induction, differentiation, or migration patterns. It is classically understood that as the neural tube separates from the epidermal layer, neural crest specified cells in the dorsal neural tissue begin to disassociate from the epithelium and delaminate from the neural tube in a process known as epithelial to mesenchyme transitioning (EMT), as shown in figure 2. It is after this point that neural crest are reported to differentiate into their various fated tissue derivatives, as is the case for melanocytes, and pigment begins to appear thereafter in the zebrafish embryo. (Krispin et al. 2011).

A)

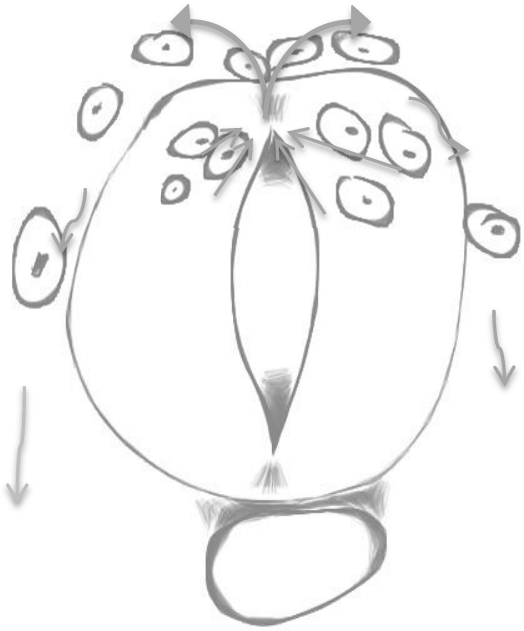

B)

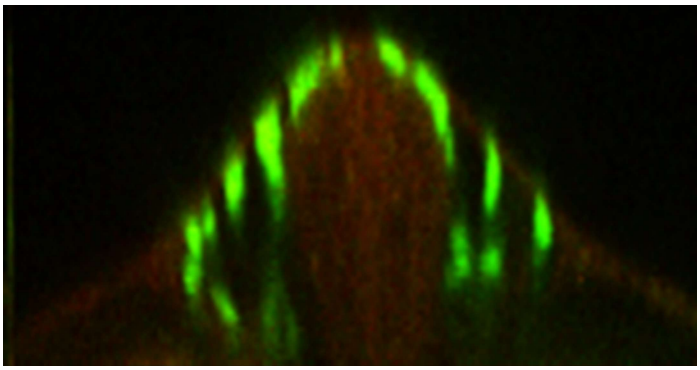

Figure 2: Epithelial to mesenchyme transition.
A) in this transverse sketch, cells of the neural epithelium disassociate from each other and with a ventral to dorsal relocation neural crest progenitors approach the transition zone, the dorsal most point of the neural tube. Upon delamination from the neuroepithelium these cells begin to differentiate and migrate to their respective destinations, ventrally and dorso-laterally migrating away from the neural tube. B)Transverse slice of actual two photon microscope image of early neural tube autofluorescence (red) and delaminating neural crest cells (cells reporting eGFP for *sox10*) migrating ventrally away from transition zone

Background

Regulation of Neural Crest Cells and Melanophore Development

In vertebrates, neural crest cells arise during neurulation, in the area between the epidermis and the forming neural tube, and migrate to their respective fated destination. Very briefly, in the induction of neural crest there is a bone morphogenetic protein (BMP) and Wnt signaling gradient that occurs near the neural groove of the neuroectoderm, effected by mesodermal and non-neural ectoderm signaling to this region. A neural plate organizes within the ectoderm, defining medially the neural ectoderm and laterally the non-neural ectoderm. The lateral reaches of the neural plate is where neural crest cells are induced and specified, in the region of gradient signal between neural and non-neural ectoderm. Transcription factors responsible for dissociation of adhered epithelial cells (EMT) activate genes that allow for the organized assembly of the neural plate and formation of the neural tube and epidermis. Cells previously located medially in the neural plate are situated in the ventral neural tube, and those neural crest specified at the lateral aspect of the plate are located in the dorsal neural tube, followed by the epithelial to mesenchymal transformation (EMT) and delamination of neural crest cells from the neural tube, requiring *slug* and *twist* activity respectively. (Gilbert, 2010). The initiation of the neural crest induction conditions requires fibroblast growth factors (*fgf*) which induce this BMP/*Wnt* gradient. In the rather expansive neural crest gene regulatory network (GRN), the cascade flows downstream of this to the neural plate border specifiers (*Zic, Pax3/7, Dlx5, and Msx1/2*) and then to the neural crest specifier genes or markers (*Slug/Snail, FoxD3, Sox9, Sox10,*

AP-2, cMyc, Twist, and Id). A cell is considered to be of neural crest lineage if it exhibits expression of any of these neural crest specifier genes. *Sox10* is known as a neural crest specifier that plays roles even in post migratory processes, directly regulating melanocyte development and neural differentiation (Meulemans D. et al., 2004).

In a maturing melanocyte, the Tyrosinase family of enzymes is responsible for melanin biosynthesis in zebrafish, including: tyrosinase (*Tyr*), tyrosinase-related protein 1 (*Tyrp1*), and dopachrome tautomerase (*dct* or *Tyrp2*). Additionally, Microphthalia-associated transcription factor (*mitfa)* is known as the "master regulator" of melanocyte identity, where knockouts of *mitfa* result in an absence of any pigment. *Sox10* expression will precede differentiation of a melanoblast, as shown in figure 3. (Mort et al., 2015)

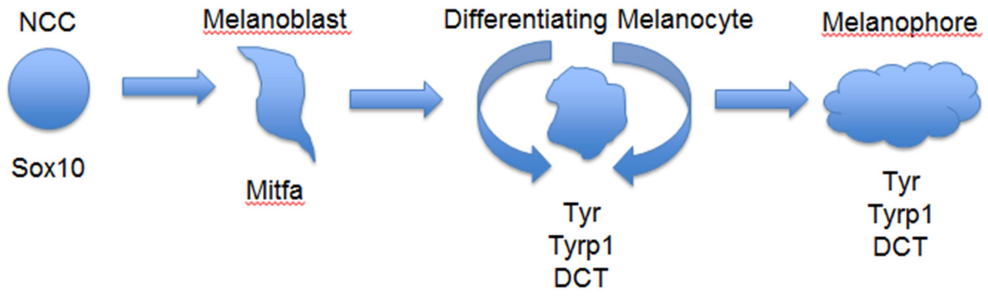

Figure 3: Developmental gene expression of melanocytes.
Neural crest cells first express sox10 and then mitfa regulates melanophore identity. As a melanoblast transitions to an adult pigment producing melanophore it begins to express the Tyrosinase family of enzymes.

In *Danio rerio*, pigment biosynthesis and deposition begins at about 24 hours post fertilization (hpf), also known as the prim-5 stage. This happens in the retinal pigment

epithelium establishing the pigment of the eyes and in mature melanocytes that proliferate and migrate throughout the zebrafish (Karlsson et al., 2001).

Pigment Suppression and Embryo Fixation

1phenyl-2thiourea (PTU) can effectively be used to prevent any pigmentation in zebrafish if it is administered in the proper dose (75 μM) well before the fish reaches Prim-5 (Karlsson et al. 2001). In zebrafish, PTU (Sigma Aldrich) is an inihibitor of melanogenesis through the inactivation of tyrosinase enzymes. In the before mentioned cycle of enzymes associated with melanin biosynthesis, Tyrosinase enzyme (*Tyr*) activity is responsible for catalyzing the reaction converting tyrosine into L-Dopa and finally dopaquinone, which is precursory to melanin pigment (Whittaker 1966). Because PTU disables tyrosinase enzymes, the development of pigment is impaired, and transparent zebrafish can be created allowing for better visualization of gene expression patterns via in-situ hybridization.

Zebrafish embryos that have undergone paraformaldehyde fixation are a valuable sample to collect for imaging as they can be stored for long periods of time and they maintain their morphological features albeit with some distortion. This process also prepares embryos and other tissue types for in-situ hybridizations and other immunohistochemical processes as the antigenic sites are left intact and available, while proteolytic enzymes are disabled. Once a clutch of embryos reach a developmental age of interest, they can be transferred into a bath of 4% Paraformaldehyde (PAF) in Phosphate Buffered Saline (PBS). Fixation protocols usually require 24 hours in 4% PAF for proper setting of the embryo, after which the embryos can be imaged or put in

100% methanol (MeOH) for storage, where they can be preserved for months prior to imaging. Though morphology is mostly maintained, fixation artifacts are inherent to the process of aldehyde fixation (Hassel et al., 1974).

When an embryo undergoes fixation morphological landmarks can move as shrinkage occurs due to the dehydration process. Morphological alterations in the tissue architecture can change the appearance of an organism, making tissue constrictions tighter or curves sharper. Registration via landmarks can be done between image sets of corresponding live and fixed specimen, using computational and image processing methods as described by Gibbs et al., 2014. Due to the fact that there are artifacts induced by fixation, it is critical to establish whether the autofluorescence of the MFCs are truly melanin based or artifacts.

Two Photon Microscopy

At the molecular level, the combined polarization (P) or dipole moment per volume of a material interacting with light is shown by the formula: $P = \chi^{(1)}E^1 + \chi^{(2)}E^2 + \chi^{(3)}E^3 + \chi^n E^n$ ... where $\chi^{(n)}$ is the nth order linear susceptibility tensor and E is the electric field vector. The linear susceptibility factor $\chi^{(n)}$ is a bulk property of a material and is equal to: $N_s\langle\beta\rangle$ where N is the molecular density and β is the hyperpolarizability. Linear processes occur when: $P = \chi^{(1)}E^1$, as in situations where a single molecule interaction occurs such as absorption or scattering. In Second Harmonic Generation (SHG) a second term is added and susceptibility is limited by symmetry on the order of excitation wavelength. Higher order nonlinearities occur to give rise to Two and Three Photon Absorption, Third Harmonic Generation (THG), and Coherent Anti-

Stokes Raman Scattering (CARS). TPEF is a third order process because the imaginary

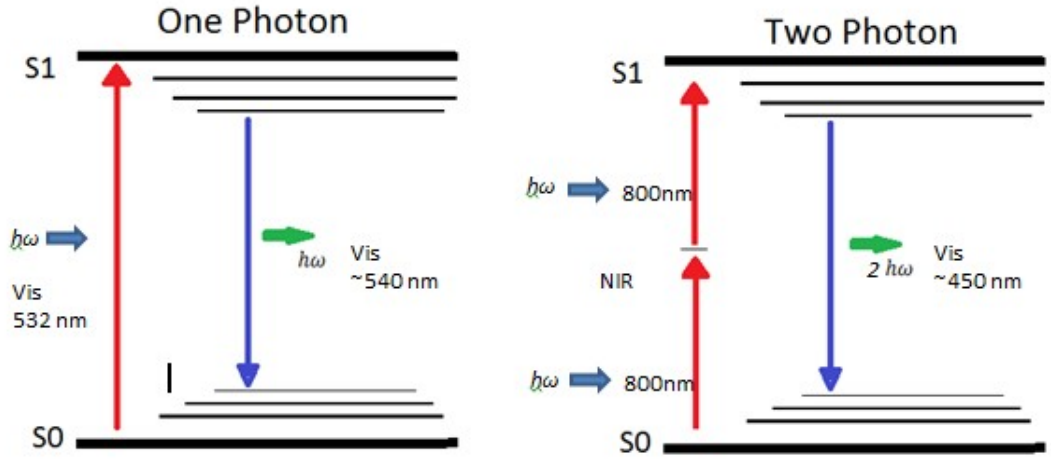

Figure 4: One photon and two photon excited fluorescence.
Jablonski diagrams detail the principles of a one-photon and two-photon process. In conventional one photon microscopy the sample absorbs one photon with sufficient energy to carry the molecule from ground(So) to excited state (S1) and then emits a fluorescence photon of similar wavelength. In two photon processes the first photon is absorbed allowing a virtual intermediate state to be achieved between S0 and S1, and the second absorbed photon fulfills the energy deficit to achieve the excited state. The resultant emission photon is the combined energy of the incident photons, with approximately half the wavelength and near twice the frequency of the individual incident photons.

$\chi^{(3)}$ is nonlinearly equivalent to the molecular absorption lineshape ($(\gamma(\omega))$ of the absorber (Shen, 1984). This Two Photon Absorption spectrum is often presented in Geoppert Mayer units of cross section (GM), where 1 GM = 10^{-50}cm^{4}s which represents the likelihood of simultaneous absorption of two photons (Drobizhev et al., 2011).

Two Photon Excited Fluorescence (TPEF) is produced when two photons are absorbed by a sample simultaneously, as displayed in figure 4. Upon absorption of these two photons, of either identical or different frequency, the sum of their energies combines to span the transition energy or bandgap. After some vibrational relaxation, a stokes shifted TPEF photon is emitted with the combined energy of the two incident excitation photons and the substrate molecule returns to the ground state. Often the

excitation light in two photon processes is in the near infrared (NIR), and the fluorescence emission is in the visible spectrum (Svoboda et al., 2006).In conventional linear optical setups, the fluorescence is proportional to the intensity of the source. Two photon excited fluorescence is dependent on the square of the excitation intensity due to the required simultaneous absorption of two photons, making it a nonlinear process, causing a steep decay of signal strength as distance from the focus increases as shown in figure 5. This is a major advantage over one photon fluorescence microscopy, as it eliminates the need for a confocal pinhole to reduce out of focus fluorescence from the desired signal originating at the focus. This signal confinement to the focal volume that is inherent of multiphoton microscopy makes it an excellent choice for optical sectioning of samples, even more so than its confocal counterparts, as this focal volume can be scanned throughout a specimen. Because fluorescence is only generated at the focus, all light can be collected as desired signal from the sample and none must be rejected by a pinhole (So et al., 2001).

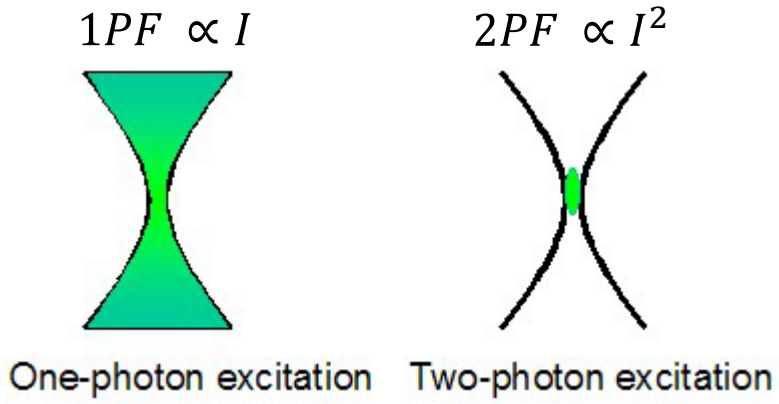

Figure 5: Signal confinement properties of 2PEF.
In one photon fluorescence, a linear relationship with intensity means a linear falloff in signal from the focus creating a cone of fluorescence emitting from the sample, requiring use of a pinhole to reject out of focus background. In two photon fluorescence the required photon density to create two photon transitions confines the the fluorescence signal to the focus.

The probability ($\Gamma(\omega) = \int_{-\infty}^{\infty} T(\omega)\gamma(\omega)d\omega$) of this phenomenon occurring is dependent on the overlap integral of $T(\omega)$ the two photon power spectrum, a portrayal of all the frequency combinations available for achieving two photon transition, and $\gamma(\omega)$ the molecular absorption line shape (Yeh, et al. 2008).

To increase the likelihood of two photon transitions, high power mode-locked pulsed Ti:Sapphire lasers are used to maximize photon density at the focus. Both spatially and temporally, these Ti:Sapphire lasers concentrate the delivery of NIR light to the sample to achieve two photon excited fluorescence. These lasers employ ultra-short pulses, often in the hundreds of femtoseconds in duration, to maximize delivered peak power to the sample while maintaining a low average power. This makes two photon microscopy an excellent option for optically sectioning thick/living biological samples as they can be probed deeply by the near infrared excitation light and high peak pulse power without causing harm to the specimen (Helmchen et al., 2005).

Ultrashort Pulse Microscopy (UPM)

The ability to visualize multiple fluorescent molecules simultaneously with excellent spatial resolution in time is the central innovation demonstrated by our ultrashort pulse microscope (UPM) system. Utilizing the broadband excitation spectrum generated by our sub-ten femtosecond pulses, multiple fluorescent labels can be excited during imaging and their emissions can be filtered accordingly. The foremost advantage of using sub ten femtosecond is the significantly increased broadband excitation. The spectrum of a sub ten femtosecond pulse would achieve a more favorable overlap with a molecular absorption lineshape than a similarly tuned narrow band 100 femtosecond pulse as displayed in figure 6 thus allowing for higher probability of a two photon

$$T(\omega) = \left| \int_0^\infty E\left(\frac{\omega}{2} + \Omega\right) E\left(\frac{\omega}{2} - \Omega\right) d\Omega \right|^2$$

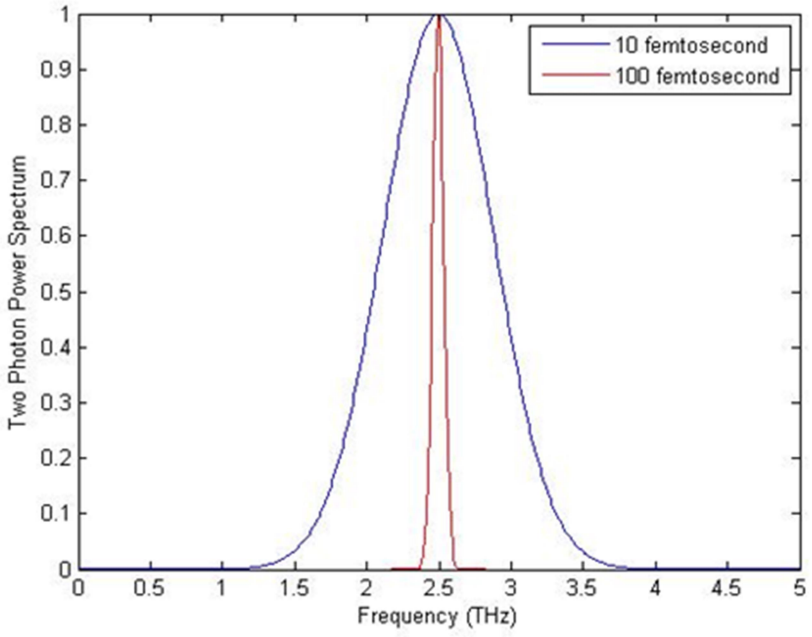

Figure 6: Two photon power spectrums.

transition.

The ultra-short pulse duration is achieved through Kerr-Lens modelocking in the Ti:Sapphire Oscillator. Briefly, a laser is composed of a highly reflective optical cavity and a gain medium. The gain medium is pumped via electric, chemical, or optical energy and population inversion is achieved. Population inversion is required for lasing to occur and is only achieved when the input energy supplied to the gain medium is sufficient to cause the cavity population residing in the excited state to far exceed the ground state. Once population inversion is achieved in a system, stimulated and spontaneous emission/relaxation is likely to occur. Spontaneous emission is when an excited state atom or molecule randomly relaxes from the excited state back to ground, releasing a photon with energy equivalent to the bandgap. Stimulated emission also occurs when an atom already resides in the excited state, yet relaxation occurs because it is perturbed by the interaction of an incident photon with energy equivalent to the band gap, causing the emission of another photon of equivalent energy and direction as the original photon. Light escapes one end of the cavity because it is less than perfectly reflective, and within a laser cavity many different longitudinal modes may exist.

Because lasing depends on oscillation of light from one end of the cavity to the other, there is constructive and destructive interference between these longitudinal modes based on the fact that the cavity length L is a multiple n of the electromagnetic wavelength λ. The resonant frequencies ν_n that exist as standing waves within a cavity are numerous and can be found by: $\nu_n = \frac{nc}{2L}$, where the speed of light is *c* and 2L is the roundtrip cavity length (Svelto, 2005). When these many longitudinal modes oscillate

freely within the cavity, their phase differences cause interference between them. Mode locking fixes the phase relationship between the modes to allow for periodic constructive interference, creating a temporally short pulse whose repetition rate is related to the cavity length.

The Kerr effect is a nonlinear optical effect in which a medium responds to an electromagnetic field, in this case an intense source of light. A Kerr medium exhibits a changing index of refraction with regard to the intensity of incident light as represented by the formula: $n(I) = n_o + n_2 I$, where n_o is the original index of refraction and n_2 is the intensity dependent component. In our system, Kerr Lensing or Kerr Lens Modelocking takes place with the use of the Ti:Sapphire crystal acting as the both a gain medium and a Kerr medium. As high intensity laser light passes through the crystal, it becomes a gradient index lens due to the optical Kerr effect, where high intensity light is

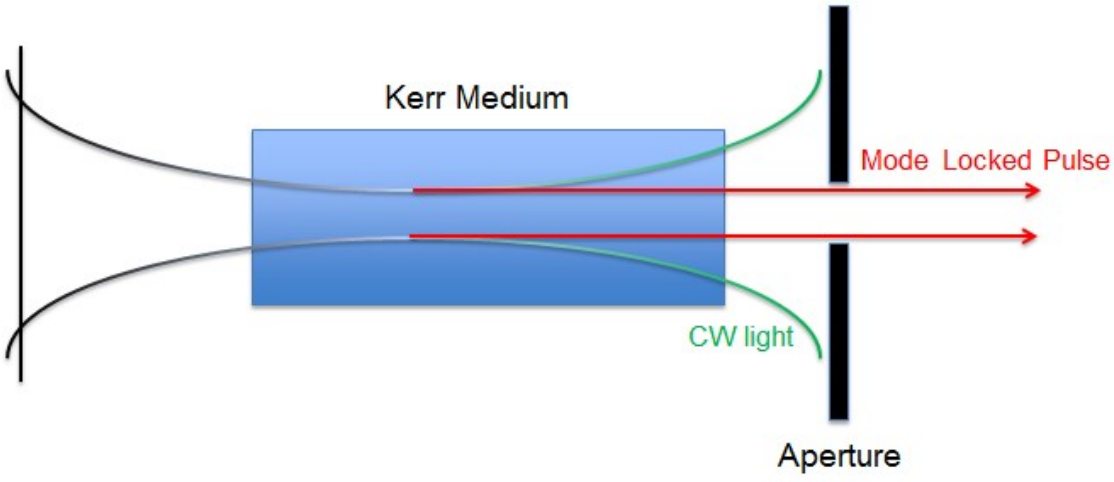

Figure 7: Hard aperture kerr lens modelocking.

focused and low intensity continuous wave light is broadened. An aperture causes loss in the low power broadened light and the focused light with high power is intensified and allowed to traverse the cavity as seen in figure 7 (Beyersdorf, 2009).

The method of Kerr Lensing shown above utilizes a hard aperture, whereas in our system a soft aperture is used. Within the resonator, curved mirrors focus both CW and pulsed laser light onto the gain crystal; however, the depth of field of a pulsed beam is much greater than that of CW light. Taking advantage of the confocal parameter differences in continuous wave and pulsed laser light, moving the stability range mirror can effectively remove much of the CW focus from the gain medium causing loss, whereas the longer depth of focus of the pulsed beam allows this light to experience the gain medium and bring about mode locked pulses. This method is called "soft aperture" because a physical obstacle doesn't generate the loss as it does when using an actual aperture.

Tissue Autofluorescence & Second Harmonic Generation

To achieve the wild type TPEF images as achieved by Gibbs et al., living tissue metabolites within each cell were taken advantage of. Within each cell there is an individual cellular metabolism that contributes to the organism as a whole. When light is absorbed by the organelles and molecules that compose a cellular metabolism, they naturally emit. This emission is called autofluorescence and it allows for label free imaging of tissues and cells. The major endogenous contributors of autofluorescence in zebrafish embryos are NADPH and flavins (Zipfel et al., 2003).

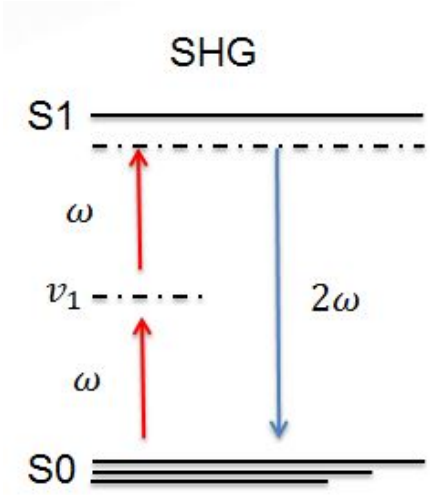

Figure 8: Second harmonic generation.
In second harmonic generation, two incident photons of exactly the same frequency combine in a lossless event to create frequency doubled light, with the same quadratic relationship to incident intensity as TPEF. In SHG, it is not necessary that excited state S1 be reached and a secondary virtual state is achieved. This means there is no vibrational relaxation as in TPEF.

The chiral, ordered structure of collagen provides another endogenous signal in the form of second harmonic generation (SHG), which is an altogether different nonlinear process. Referring back to the molecular polarization (P) of a sample, in a $\chi^{(2)}$ process such as SHG the bulk properties are determined by the tissue architecture on the order of the excitation wavelength. If the tissue presents a locus, an area lacking inversion symmetry, and its dipole aligns with the focal volume of the source, then SHG signal will be restricted to this area where $\chi^{(2)} \neq 0$ (Chen et al., 2012).

TPEF is not lossless, due to vibrational relaxation. In SHG however, the incident photons are identical in frequency and they are not absorbed, but scattered elastically and combined in a lossless event. The incident photons are exactly half the frequency of the resultant second harmonic generation, as shown in figure 8, thus this phenomenon is called frequency doubling, as the excitation light is effectively doubled in energy (Band,

2006). SHG has a quadratic relationship to the intensity of incident light much like two photon processes, so it also exhibits signal confinement making it excellent for optically sectioning tissues. (Cox et al., 2003). SHG, autofluorescence, and TPEF can be epifluorescence-collected from the sample and separated by a series of dichroic mirrors and emission filters before detection.

Transgenic Reporter Lines

Transgenic reporter lines can be imaged live to reveal the spatio-temporal profiles of gene expression. As previously mentioned, the transcription factor *sox10* and identity regulator *mitfa* are possible genetic markers of the MFC population. Time lapse imaging of both gene expression patterns was made possible by multiple generous contributions from the zebrafish community.

The Green Fluorescent Protein (GFP) gene was discovered when jellyfish *Aquorea Victoria* was shown to exhibit a fluorescence when cells were exposed to UV light (Davenport et al., 1955). Not long after, the gene was cloned and inserted under the control of a promoter of a gene of interest in another species, allowing tracking of that gene expression at the cellular level as a fluorescent protein would be transcribed each time the gene of interest was transcribed. The first stable line of GFP transgenic zebrafish inserted after a zebrafish promoter was created by Long et al., 1997, and since then many more lines have been created with other different genes of interest. Other natural fluorescent proteins have been utilized in a similar fashion for molecular marking, like blue, red, and yellow fluorescent proteins (Kremers et al., 2011).

Several mutations of the GFP reporting protein have led to variations allowing different utilities, such as differing absorption and emission spectra, as well as increased quantum efficiency. An improved mutant of GFP, Phe-64→Leu, Ser-65→Thr, referred to as enhanced Green Fluorescent Protein (eGFP), has been shown to emit more strongly than its predecessors (Cinelli et al., 2000). The eGFP fluorescence displayed by these transgenic lines can be imaged via our UPM system due to the fact that the cross section is ample within our range of excitation for two photon transitions to occur. To view both cellular autofluorescence and eGFP fluorescence two detection channels are utilized, and eGFP reporter signal can be overlaid on label free tissue for localization of reporters within tissue morphology.

Project Aims

Aim 1) Establish Relationship Between Pigment Synthesis and Midbrain Signal

Because there is a chance that this population of potential MFCs is in fact an autofluorescence artifact, further characterization is required. To rule out this possibility, pigment suppression experiments can be conducted to indicate whether the autofluorescence signal is indeed related to pigment synthesis.

Approach:

If this autofluorescence signal is related to melanin biosynthesis, then the signal should decrease with PTU treatment in a dose-dependent manner. A preliminary experiment detailing the ability of PTU to reduce pigment/signal in this region of the neuroepithelium was performed. In this experiment, the PTU dose dependent response of the autofluorescence signal is measured in fixed

embryos at the 27 hpf point where preliminary embryos were seen to present with the autofluorescence signal as mentioned by Gibbs et al. 2014.

Aim 2) Confirm Presence of Autofluorescence Signal in WT Neuroepithelium

A temporal profile of these MFCs must be defined to confirm and extend early results of Gibbs et al. (2014). The observed population resides in the dorsolateral hinge points in the developing neural tube at some point after 24 hours post fertilization (hpf). An autofluorescence signal could be demonstrated within the midbrain epithelium, excited by ultrashort pulses, to confirm early results.

Approach:

Fixed WT embryo experiments were conducted at time points of interest in the zebrafish development to highlight autofluorescence as shown in Gibbs et al. Ultrashort Pulse Microscopy (UPM) was used to image a number of fixed embryos at these timepoints to display any autofluorescence within the midbrain with a similar setup to those as shown by Gibbs et al, 2014. Investigation of the neuroepithelium of wild type embryos and confirmation of a strong autofluorescence signal in the dorsolateral hinge points of the developing midbrain was endeavored by both fixation experiments and time lapse imaging experiments. Because detection of this population will first occur between 24 hpf and 28 hpf according to Gibbs, et al (2014), time lapse experiments were started well before 24 hours post fertilization (hpf), with images of the midbrain region acquired every 20 minutes until the embryo has passed 28 hpf in development.

This autofluorescence signal is the defining feature of the MFCs within the neuroepithelium, and outlining the general timeline of origination and migration of this population will aid in further identification experiments.

Aim 3) Determine the Genetic Identity of Population in Question

The identity of these cells can be determined by visualizing mRNA transcripts at the cellular level, where reporting of genes marking neural crest or pigment identity could suggest identity via colocalization with MFC signal. Though this signal could have a variety of different fluorophore sources, those demonstrated to strongly fluoresce, such as melanin, will be probed first. The lineage of these MFCs can be characterized using fluorescence reporting of the gene expression necessary for induction and proliferation of melanophores. The spatio-temporal profile of the expression of neural crest marker *sox10* and melanophore identity regulating gene *mitfa* must be observed to highlight possible co-localization of these reporters and the autofluorescence signal in question.

Approach:

Not only will time lapse imaging experiments of WT embryos be performed, but also of transgenic lines of zebrafish reporting with eGFP for *sox10* and *mitfa* expression in the developing zebrafish cranial region. Periods of development to be visualized were decided upon based on preliminary results of WT studies and the developmental traits of zebrafish concerning melanocyte onset and differentiation. Ultimately, both *sox10* and *mitfa* were studied from 24-30 hpf, but notably *sox10* expression was imaged for a much larger duration of time as it has activity for much of the development.

Utilizing UPM, this study will assess the hypothetical existence of another cranial neural crest cell population in zebrafish through defining the lineage of the MFCs to be neural crest derived or otherwise. This proposed study will challenge and enhance current understanding of the zebrafish neural crest and perhaps characterize a separate line of pigment cells exhibiting an evolutionary trait of their ancestors.

MATERIALS AND METHODS

Ultrashort Pulse Microscopy

All imaging was conducted using our broadband UPM system in which pulses centered at 800 nm (figure 9) from a mode-locked Ti:Sapphire oscillator (Femto Lasers, Vienna Austria) pumped by a 5-W Frequency Doubled Verdi laser (Coherent Radiation, Palo Alto Ca) were directed through dispersion compensating mirrors (GSM 270, Femtolasers) and raster scanned across a 635 nm short pass dichroic mirror (Chroma,

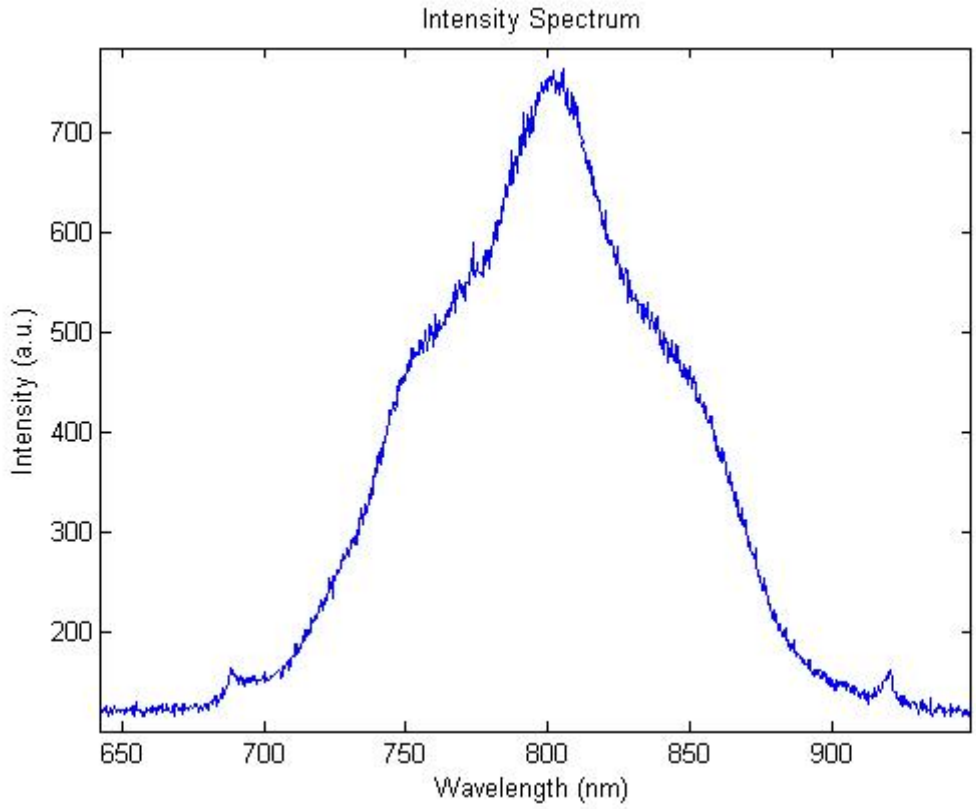

Figure 9: Intensity spectrum of modelocked sub-ten femtosecond pulse.
Intensity spectrum of modelocked laser pulses achieved by our Ultrashort Pulse Microscopy system. Sub ten femtosecond pulses generate an optimal FWHM bandwidth of 133 nm centered at 800 nm from OceanOptics Spectrometer.

Bellows Falls, VT) and also the back focal plane of a Plan/Apochromatic 20X 1.0 N.A. water immersion objective (Zeiss) by a galvanometer-driven x–y scanner (Series 603X, Cambridge Technology, Watertown, MA) within an Axiovert 100 microscope (Zeiss).

Two photon excited fluorescence (TPEF) signals were separated by dichroic mirrors and passed through various emission filters and then detected by a photomultiplier tube (PMT) as shown in Figure 10. Labview automation (National Instruments, Austin, TX) handled data acquisition and stacks composed of x-y images 256x256 pixels were collected and processed in Matlab. (Wu, et al. 2011). The lateral and axial resolution of a two photon fluorescence microscope is generally considered to be half as good as conventional confocal setups due to excitation wavelengths of roughly double that used in confocal microscopy. Using the equations $r_{xy} = \frac{.46\lambda}{NA}$ $r_z = \frac{1.4n\lambda}{NA^2}$ with water and assuming an 800 nm excitation wavelength the lateral resolution would be ~0.368 microns and the axial ~1.49 microns.

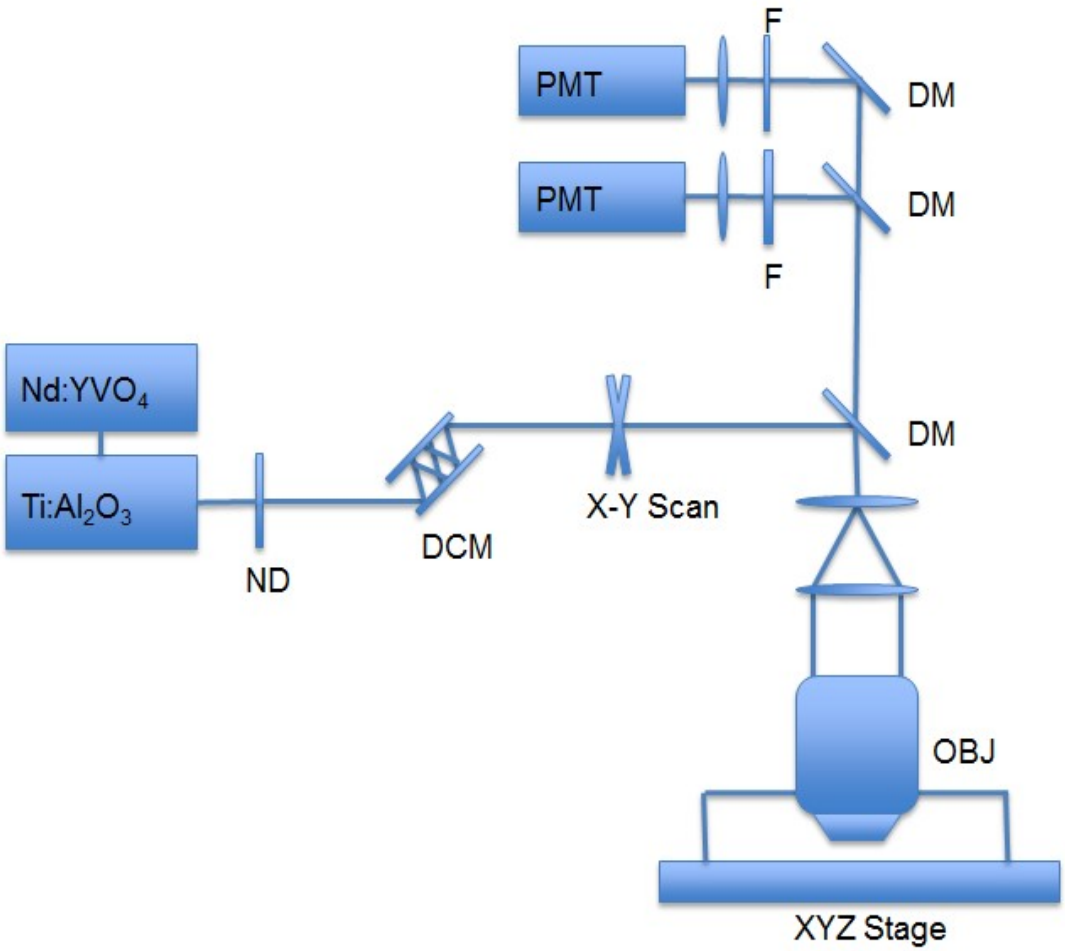

Figure 10: Schematic of ultrashort pulse microscopy system.
A schematic of the ultrashort pulse microscopy system. A 75 MHz ti:sapphire oscillator puts out sub ten femtosecond pulses that are directed to a neutral density (ND) filter, dispersion compensating mirrors (DCM) and onto the back of the objective using X-Y scanning galvanometer driven mirrors. When TPEF signals are being acquired the signals are directed through a dichroic mirror (DM) and emission filters to the photomultiplier tubes for detection.

PTU Pigment Suppression Experiment with Wild Type Zebrafish Embryos

All zebrafish care and husbandry were conducted as required by standard protocols of the field (Westerfield, 2000). Wild type embryos of AB stock were crossed and embryos were kept at 29^{o}C for the duration of pre-fixation development. Embryos of the same clutch were raised in separate petri dishes containing the following different concentrations of PTU (0 μM, 20 μM, 40 μM, 56 μM, and 75 μM which was the effective 0.004% concentration used to suppress pigment). Embryos were raised to 27 hpf and fixed in 4% PAF in PBS solution for 24 hours at 4^{o}C, and transferred to a methanol solution for storage before imaging. Prior to imaging, zebrafish embryos were rehydrated in a stepwise methanol to water transition, of 100% , 75%, 25%, and 0% MeOH in water dilutions. Fixed embryos were mounted in the dorsal upright position using a well made by a p200 pipette tip in 1.2% agarose gel that was then covered with water within a petri dish for use with a water immersion objective. Embryos were imaged at multiple depths via our ultrashort pulse microscopy system, spanning the dorsal-lateral reach of this presenting signal within the neuroepithelium, as shown in Figure 14. Measuring from the most dorsal point of the embryo into the midbrain, images were taken of each embryo at 75, 90, 105, 120, and 135 micrometers in depth, chosen as representative depths at which the autofluorescence signal had presented. During this PTU experiment, a program to calculate the average pixel intensity in the region of interest was used and values were recorded at each depth for each embryo, as shown in Figure 11. As a built in control, average pixel intensity of areas of tissue

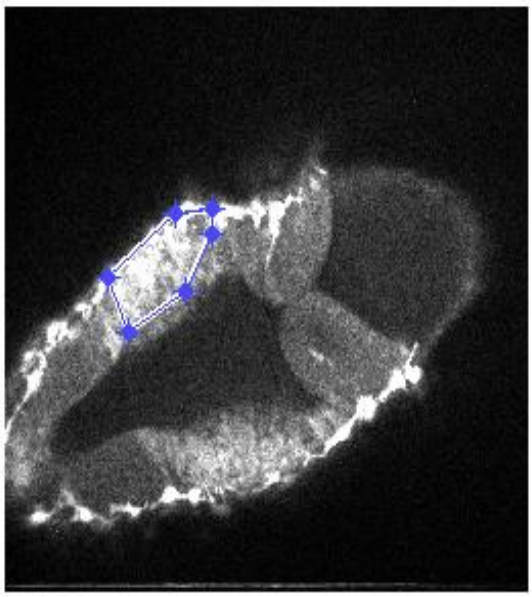

Figure 11: Masking tool to select a region of interest.
A masking tool was utilized to select a region of interest and a non-interest area of neuroepithelial tissue when calculating signal intensities in PTU treated fish.

outside of the ROI were taken as well. To image wild type autofluorescence the dichroic mirrors and filters were arranged such that a 630 long pass dichroic directs epifluorescence through a BG-39 (510nm ±105nm) emission filter (ThorLabs), onto a single photomultiplier tube (PMT) detector.

Once the datasets from each embryo were collected, 10 embryos per concentration of PTU, with five concentrations, allowing 50 degrees of freedom, the T-values and Pearson Correlation Coefficients were calculated at each depth to portray the relationship between PTU concentration and autofluorescence signal intensity in the ROI and elsewhere in the neuroepithelium to find a negative or positive correlation if one existed.

Wild Type Zebrafish Imaging Experiments

Fixed WT Embryo Imaging

To further investigate the early observations of Gibbs et al, 2014, we characterized the developmental stages at which this signal could be observed in fixed embryos. To do this, AB wt embryos were raised at 29^{o}C until matured to 24, 25, 26, 27, 28, and 30 hpf , fixed in 4% PAF, rehydrated, and mounted as previously described. Image stacks were taken with 70 images total, starting at the surface of the embryo and stepping incrementally 3 microns axially into the sample with a total penetration depth of 210 microns. Thresholding was applied to the image stacks in Matlab, the dimensions being 256x256x70 voxels and were then scaled in FIJI to account for the three micron z-resolution of the voxel. Image stacks were compiled to create three dimensional datasets by which lateral and transverse slices can be taken to further investigate the pervasion of autofluorescence signal in the neuroepithelium.

Timelapse Imaging of Whole Mount Live Zebrafish

To image WT embryos live at the time points of interest, AB WT embryos were raised and maintained with standard protocols. Once well past the 18 somite stage, live embryos were dechorionated and mounted in the upright dorsal position in 1.2% agarose (Figure 12), but not until being treated with a Tricaine anesthetic to reduce motion artifacts, and covered with low melt agarose. The zebrafish water bath was kept at 25^{o}C using a controlled hotplate. TPEF was collected with the same BG-39 filter as with WT fixed embryos, every twenty minutes from 24 hpf to 28 hpf, then the embryo was

removed and fixed as previously described. After fixation this embryo was imaged again to compare the presence of autofluorescence signal in the midbrain epithelium.

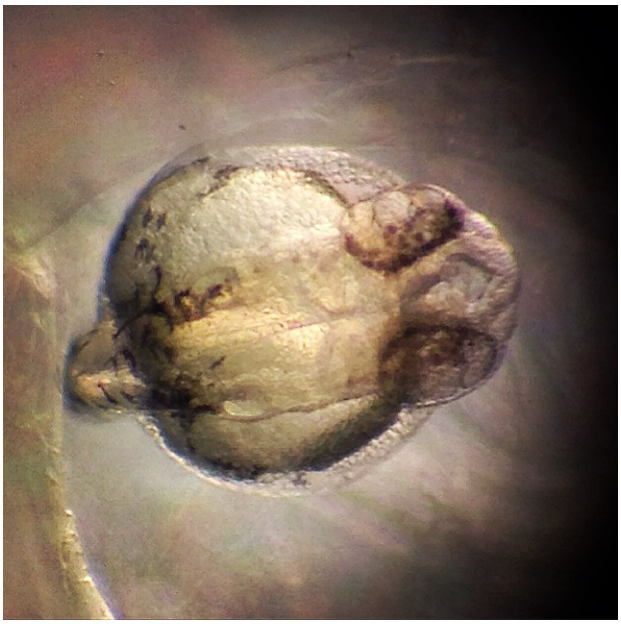

Figure 12: Dorsal view of larval zebrafish.
Dorsal view of larval zebrafish embedded in agarose gel. Zebrafish will be kept at 25 ^{o}C for duration of timelapse imaging via a controlled hotplate and anesthetized via Tricaine to prevent motion artifacts.

Transgenic Reporter Imaging Experiments

To observe spatio-temporal expression patterns of the *sox10* neural crest marker, the Marianne Bronner lab from the California Institute of Technology provided transgenic reporter Tg(-4.9sox10:eGFP) line in the form of viable embryos that have been raised to adulthood and maintained in our facilities (Dutton et al., 2008). The David Parichy Lab at University of Washington also provided a transgenic reporter line for *mitfa*, the Tg(mitfa:GFP-w47) line in the form of adult fish (Curran et al., 2010). Animal husbandry practices were performed to obtain embryos that were screened for eGFP fluorescence. Both of these lines were imaged under the same parameters as for the WT live embryo, but with a few differences. Because these fish were reporting eGFP for expression of *sox10* and *mitfa*, the epifluorescence collection setup was configured to collect a different emission spectra centered at 509 nm and is displayed in Figure 13. This eGFP fluorescence could potentially be overwhelmed by melanophore development at 24 hpf, so fish were treated with 0.004% PTU to suppress this interfering pigment production. Tg(-4.9sox10:eGFP) embryos were imaged live from the 18 somite stage until 40 hpf, while Tg(mitfa:GFP-w47) embryos were imaged from 24 hpf to 28hpf.

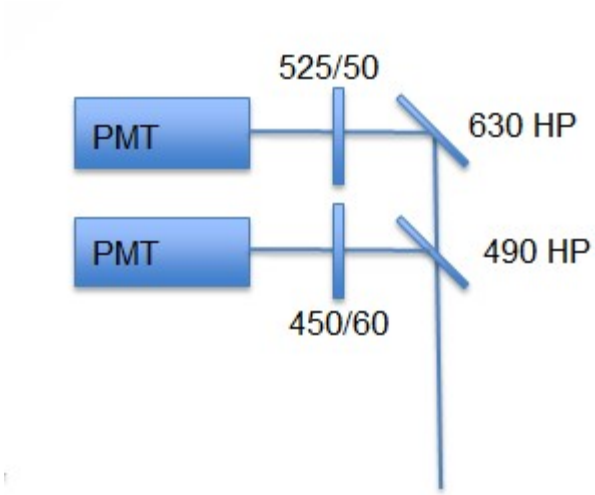

Figure 13: eGFP imaging.
For eGFP imaging, fluorescence is directed first onto a 490 nm High Pass Dichroic Mirror, where autofluorescence is directed to a 450 nm ±60nm emission filter. Longer wavelengths pass through onto the 630 High Pass mirror and green fluorescence is filtered by a 525 nm bandgap filter ±50 nm to target eGFP collection with emission maximum at 509 nm

RESULTS AND DISCUSSION

Wild Type Zebrafish Experiments

PTU Experiments

A linear relationship between PTU concentration and average signal intensity in our regions of interest has been demonstrated in each trial and at each depth as shown in Figure 15. The pearson correlation coefficient magnitude has been found to be as high as -0.892 at 90 microns depth, with this strong correlation testing at 99.99% confidence (t-value of 13.69 at 50 degrees of freedom). At 75 microns depth, the correlation coefficient was -0.865 with t-value of 11.96. This result indicates a negative relationship between the concentration of PTU and the TPEF intensity of the MFCs. As an internal control, autofluorescence signal was measured similarly outside of the ROI to observe whether the normal cellular autofluorescence was not diminishing with PTU as well. A control correlation of -0.5732 was found that also tested at 99.99% confidence suggesting a slight change in normal autofluorescence with PTU treatment. This is a much weaker correlation than original experimental results, and additionally the ratio of pixel intensities must be considered as well. In control embryos, the region of interest intensity was usually 2-5X greater than that of the cellular autofluorescence, whereas in PTU treated embryos the ratio was close to 1:1. While this doesn't prove the genetic identity of this cell population, the dose graded signal's response to PTU suggests a pigment cell's presence.

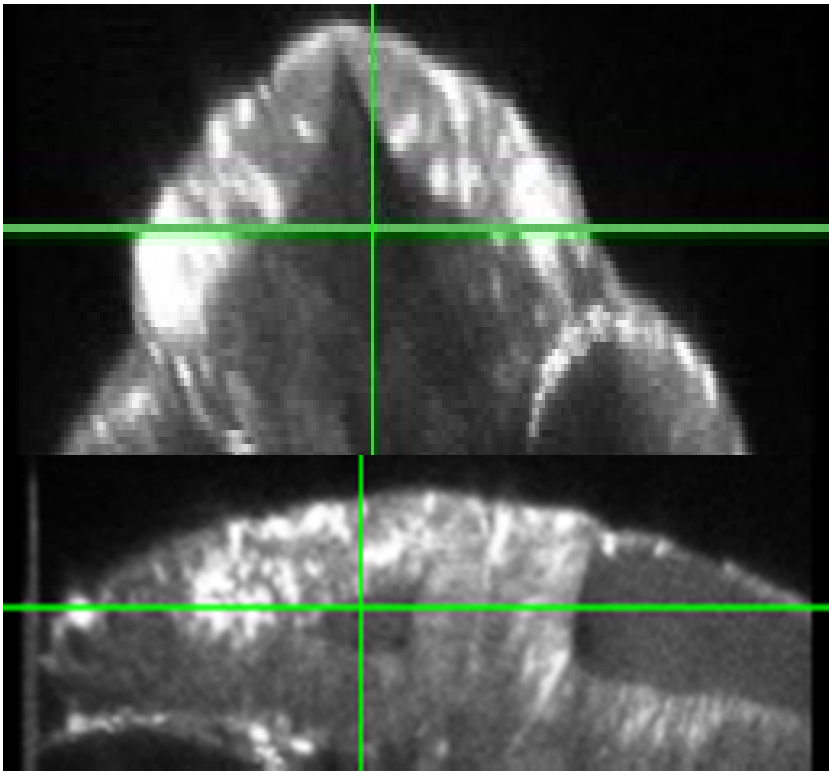

Figure 14: Control WT embryo.
One of 50 embryos fixed and imaged during PTU concentration trials. This particular embryo was a control that was not treated with PTU and displays a strong autofluorescence signal (2-5X stronger than surrounding tissue fluorescence) within the neuroepithelium in both transverse and lateral views. This signal intensity faded as concentration of PTU increased.

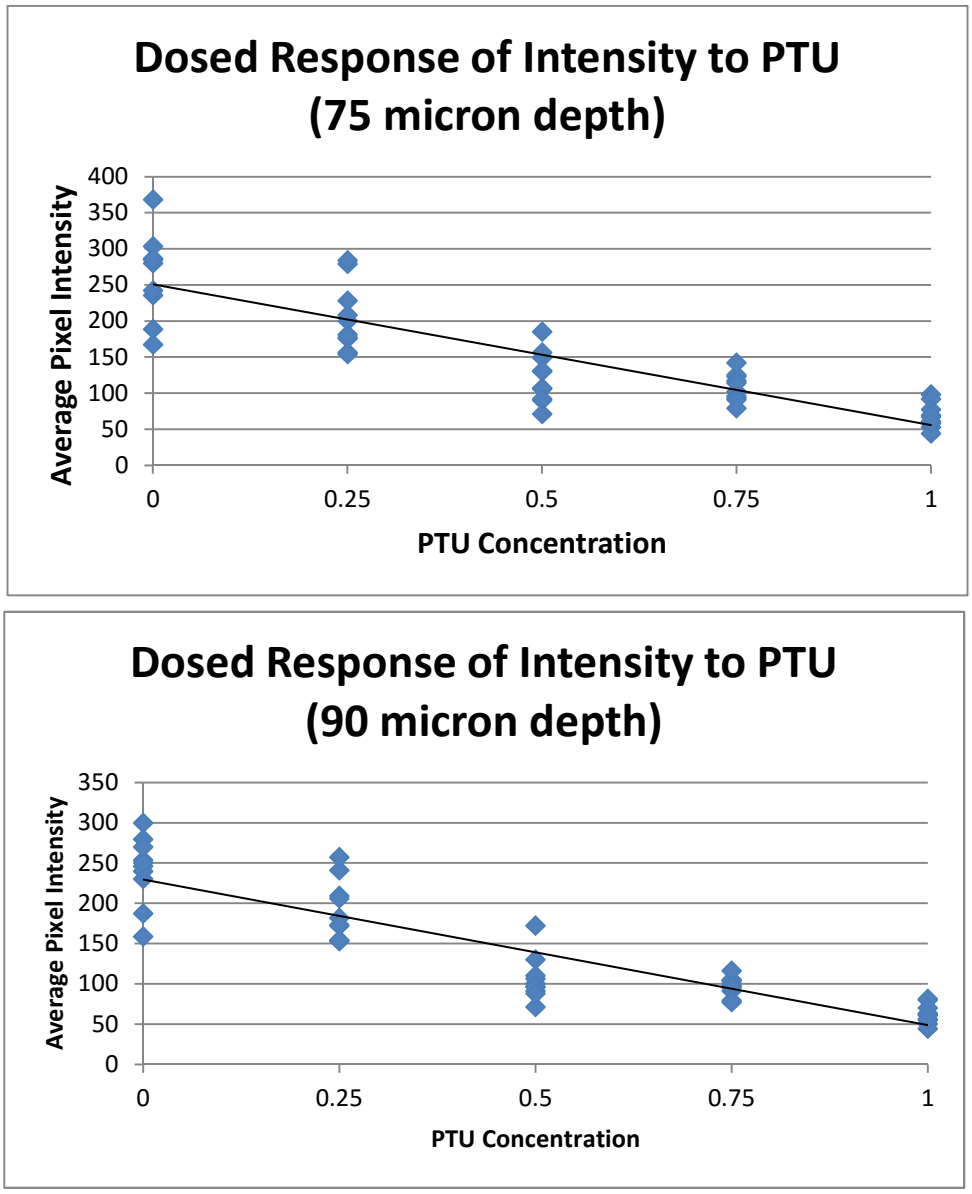

Figure 15: Linear correlation between PTU dosage and ROI signal intensity.

Confirmed Autofluorescence in Fixed WT Embryos

To extend the observation made by Gibbs et al., 2014, WT embryos were fixed at several timepoints of interest, especially from 24-28 hpf. Below are images that show the difference between a 24 hpf embryo, which does not exhibit the intense autofluorescence signal, and a 27 hpf embryo that does. It should be noted that autofluorescence signals residing near the dorsal most edges of the neural tube are to be expected, as they are known to be delaminated crest cells that are differentiating into melanophores and migrating dorsolaterally away from the transition zone. The cells of particular interest are signal baring cells pervading the neuroepithelium within the dorsolateral hingepoints and slightly above the midline in the dorsal epithelium of the midbrain. Below are representative images of fish at different timepoints in Figures 16 - 20.

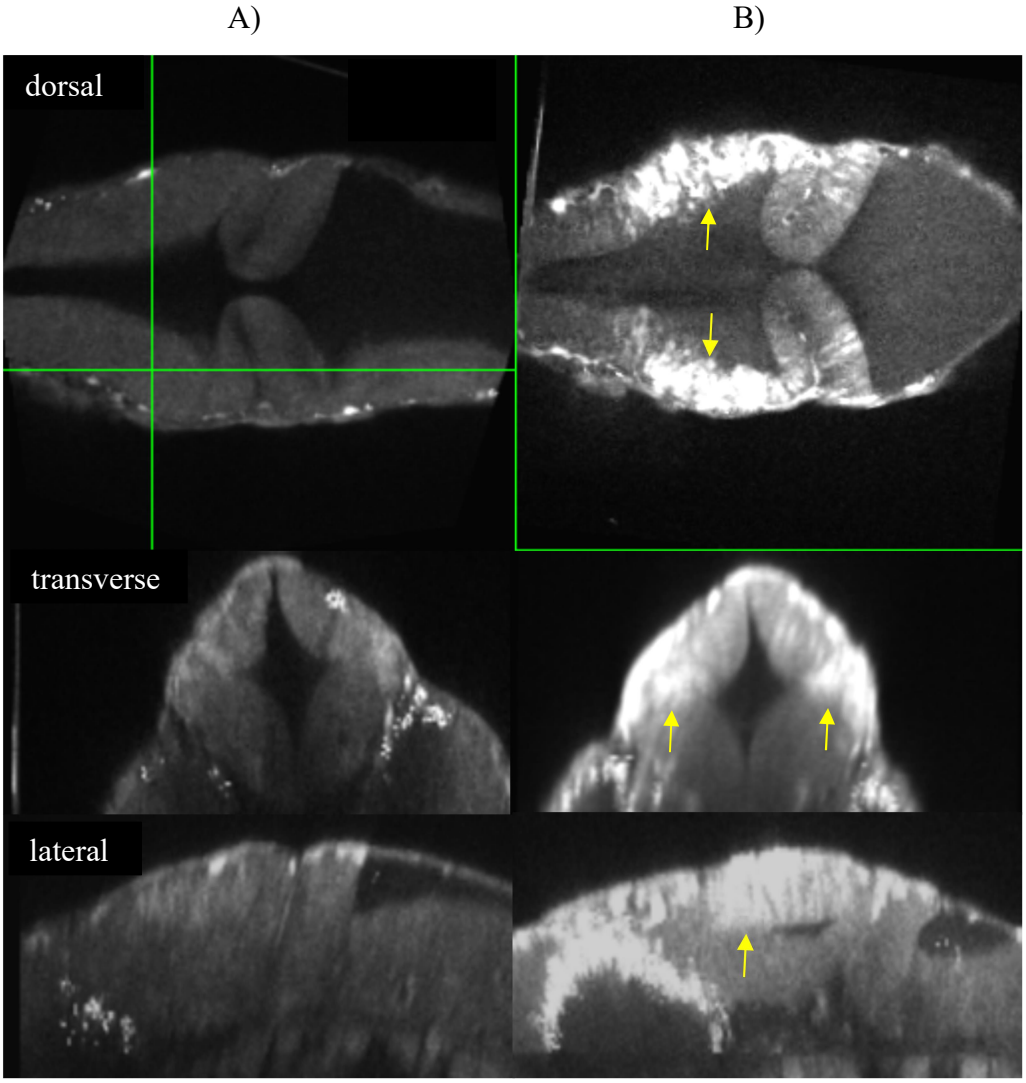

Figure 16: Dorsal images of the midbrain region of fixed WT embryos.
Preliminary dorsal images of the midbrain region of fixed embryos at a) 24 hpf and b) 27 hpf. Note the difference in intensity in regions similar to findings by Gibbs et al. (2014) The signal in question presents anterior to the midbrain hindbrain constriction and spans the neuroepithelium reaching as far as the apical constriction. Transverse slices display a strong signal intensity within the dorsolateral hingepoints and lateral slices show the same signal's invasion in f).

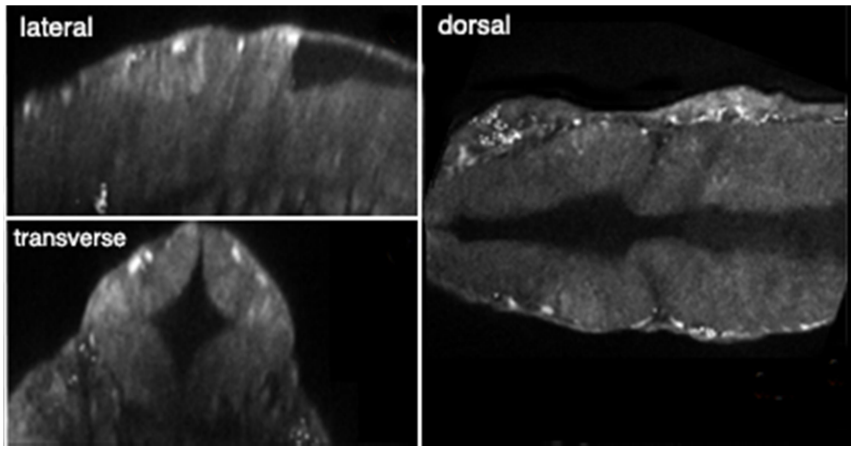

Figure 17: 24 hpf WT fixed embryo.

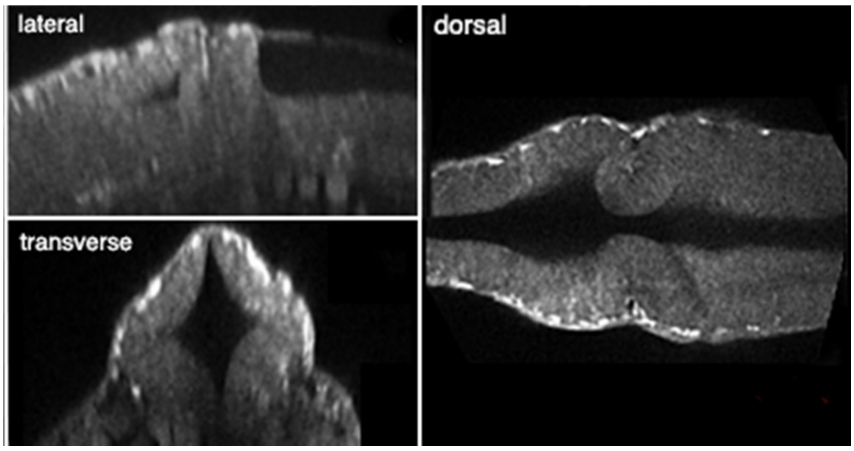

Figure 18: 25 hpf WT fixed embryo.

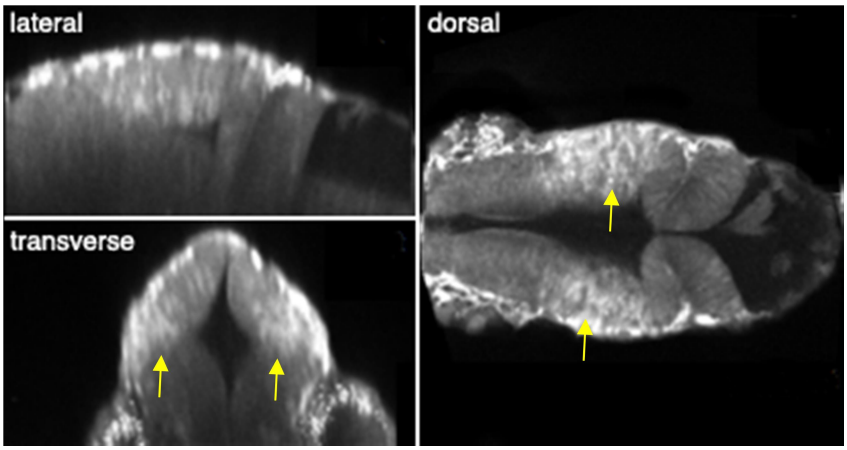

Figure 19: 26-27 hpf WT fixed embryo.

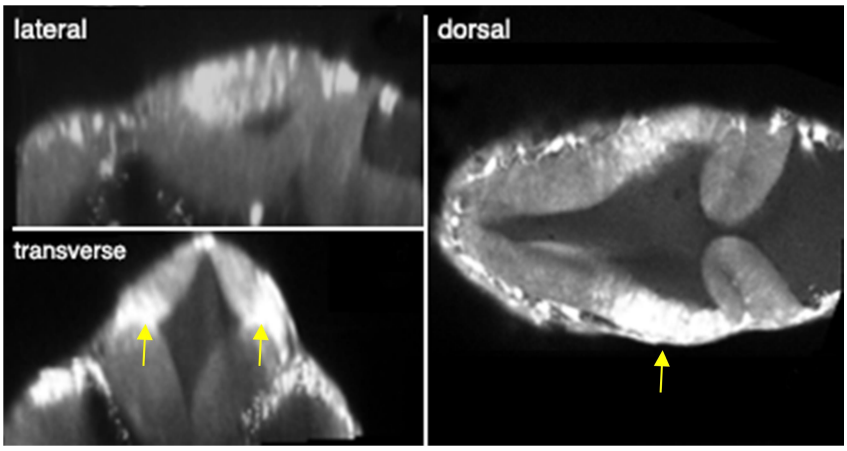

Figure 20: 27-28 hpf WT fixed embryo.

Wild Type Time Lapse Live-Imaging

Next we sought to characterize the spatio-temporal progression of the autofluorescence signal in question and time lapse imaging of live wild type embryos was conducted. In Figure 21 is a representative time lapse set of a wt embryo.

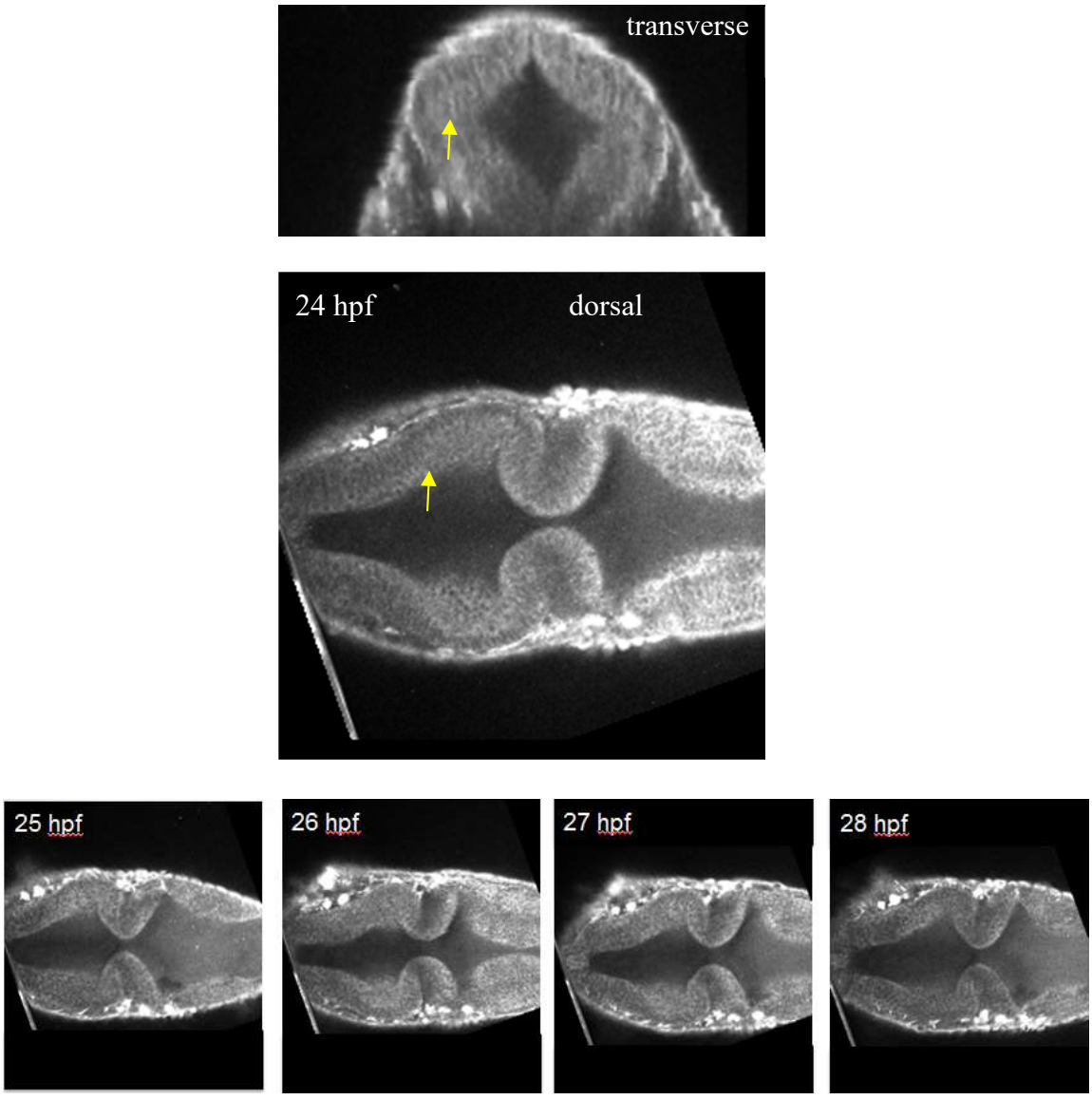

Figure 21: Time lapse imaging of WT embryo.

We did not observe MFCs in live embryos, from 24 hpf and proceeding through 28 hpf , in contrast to the PTU experiment. Once this live time lapse fish reached 28 hpf, the developmental stage at which ROI signals were at their peak strength in fixed WT embryos, it was immediately fixed via paraformaldehyde immersion and then re-imaged below in Figure 22.

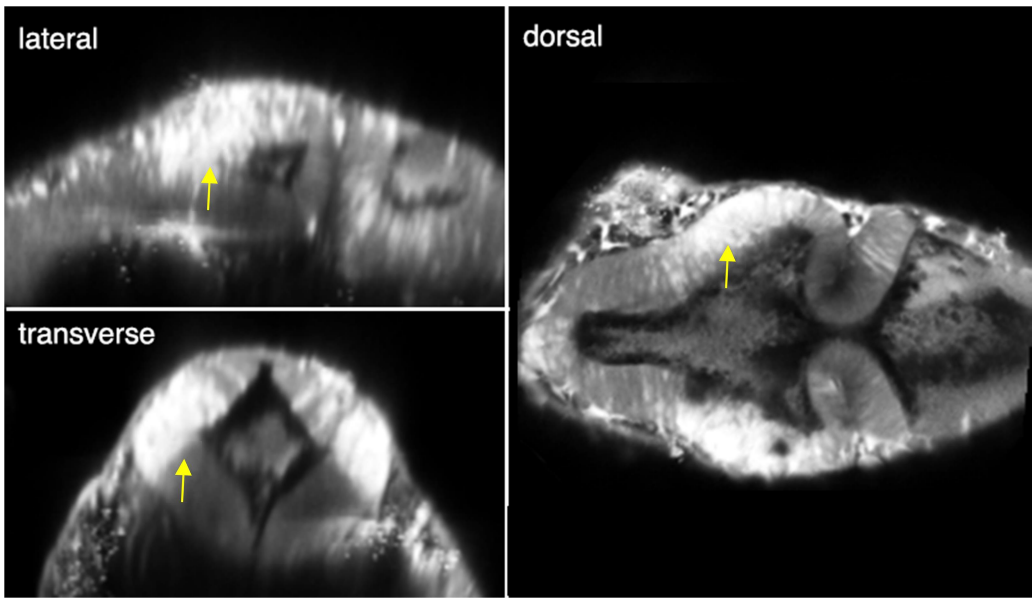

Figure 22: Imaging post fixation and live imaging.
MFCs may be result of fixation artifacts, as this fixed embryo exhibits the characteristic signal shortly after exhibiting an absence of the signal while it was imaged live. Anterior at right.

The results generated in the wild type embryo experiments are inconclusive. While the PTU concentration experiments potentially posit a relationship between pigment biosynthesis and the autofluorescence signal at question, they do not solidify the identity of the signal source. This is due in part to the possibility that the autofluorescence signal is simply an artifact of fixation where PTU treatment could be affecting this process or the substrate of the process. PTU affects the tyrosinase activities in the organism it interacts with, tyrosine amino acids being a major contributor to

autofluorescence signals. The concentration used in zebrafish experiments is commonly 0.003% PTU to suppress the pigmentation. This concentration has been found to be goitragenic as it disables thyroxine (T4) activity in the developing thyroid in zebrafish. Amongst other side effects of goiter inducing drugs in zebrafish are delayed or disrupted hatching, morphological mutation, and retardation of neural crest development (Elsalini et al., 2003).

Fixation could be concentrating the metabolite substances that are the source of autofluorescence in fixed embryos. The addition of PTU reduces metabolic activity, as its goitragenic activity induces hypothyroidism and thus a diminished metabolic rate perhaps even in zebrafish brain. During zebrafish development in the pharyngula stages, the developing tectum experiences an increase in proliferation and growth along with a boost in cellular metabolic processes during this period (Nakamura et al., 2001). With reduced metabolic rates there would be a decrease in NADPH and the flavins involved in metabolism reactions throughout an organism, and especially in the developing tectum. This would reduce an autofluorescence signal, based on the notion that PTU slows brain metabolism and thus reduces autofluorescence contributors. Flavins are founded on the substantive blocks of pteridine, which is a yellow pigment substance that is also deposited by xanthophores, a pigment cell derivative of the neural crest. Other potential causes are the PTU induced reduction in the substance reacting with paraformaldehyde to give the autofluorescence signal.

The time lapse imaging experiments would seem to effectively prove that the autofluorescence signals must be due to fixation, perhaps by one of the previously mentioned mechanisms, as the signal is absent up to the point that fixation has occurred. It is most likely that there is a reaction occurring between the aldehyde and amines or proteins in the brain to generate this autofluorescence signal. Fixative-induced autofluorescence is generally considered to be evenly distributed across tissues, while the signal observed in WT fixed zebrafish embryos is densely concentrated in a specific region of the brain, perhaps due to an accumulation of amines or proteins (Kiernan et al. 2004). Perhaps a more exotic source of the signal could be brain lipofuscins, granular aging pigment that accumulates in the brain of many vertebrates, even humans (Goyal, 1982). These pigment cells have not been observed in zebrafish to date, though they have been used in aging studies (Kishi et al., 2003). Lipofuscins are a byproduct of aging, specifically the decomposition of red blood cells, where granular pigment molecules of a brown color are deposited. They are known to be prevalent in the central nervous system, concentrated in neurons and glial cells (Kiernan et al). The autofluorescence signal observed by our ultrashort pulse microscopy could be the first time these senescence molecules have been detected in zebrafish, their conglomeration due to fixation strengthening their fluorescence signal.

Transgenic Zebrafish Experiments

Time Lapse Live Imaging of -4.9sox10:eGFP Line

Time lapse imaging was conducted to see if the neural crest lineage marker *sox10* could be observed in the neuroepithelium, indicating the differentiation of neural crest progenitors before delamination. Results of time lapse experiments spanning 17 hours post fertilization to 30 hours are displayed in Figure 23.

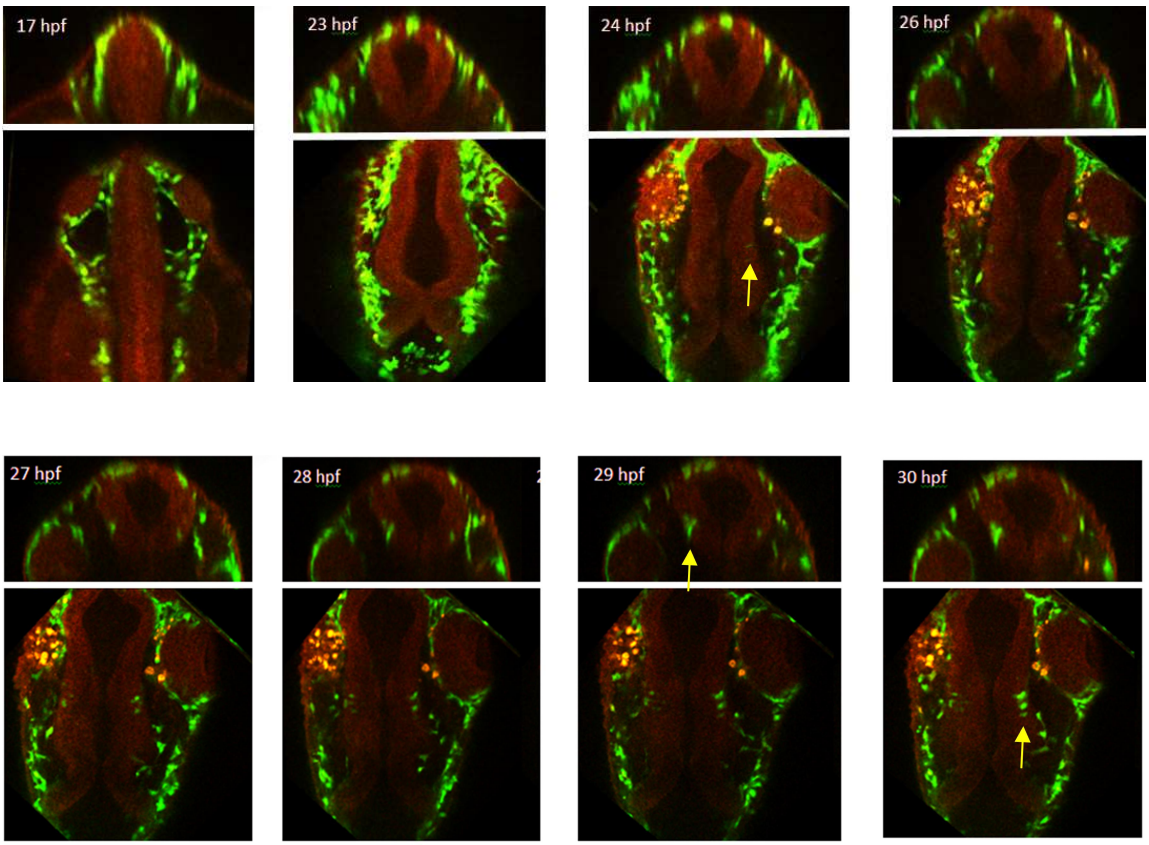

Figure 23: *sox10* reporting 17 hpf to 30 hpf.

In the images displayed, the onset of neuroepithelial *sox10* expression occurs at the prim-5 stage, about 24 hpf. In each transverse slice after 24 hpf, a population of cells

reporting for *sox10* begins to proliferate just below the dorsolateral hingepoints of the neuroepithelium. These cells migrate frontally within the midbrain epithelium, as their distinct patterning is seen to move toward the eye and nasal cavity, and dorsally as they reposition within the dorsolateral hingepoints near 32 hpf. Orthogonal sections from another embryo show the burgeoning neuroepithelial signal on the right and left side of the ventral neural tube at early stages of the signal (24 hpf) in Figure 24.

The signal presents as a singular cell or cluster of cells witin the anterior wall of the neural tube. The signal proliferates into three clusters and migrates as shown by the following image of a 30 hpf live *sox10* embryo in Figure 25.

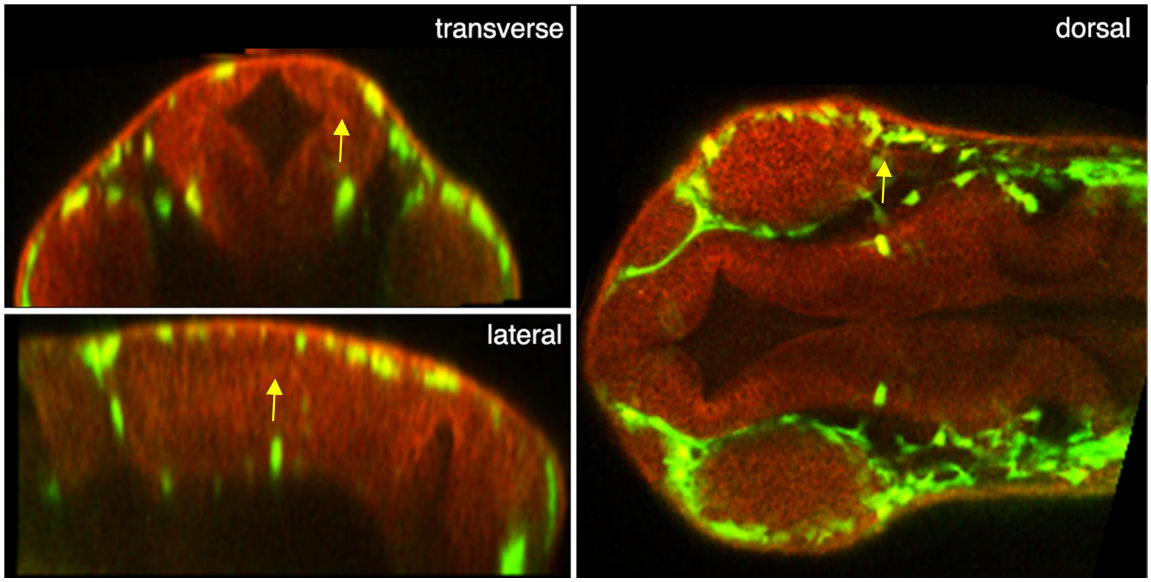

Figure 24: *sox10* reporting 24 hpf.

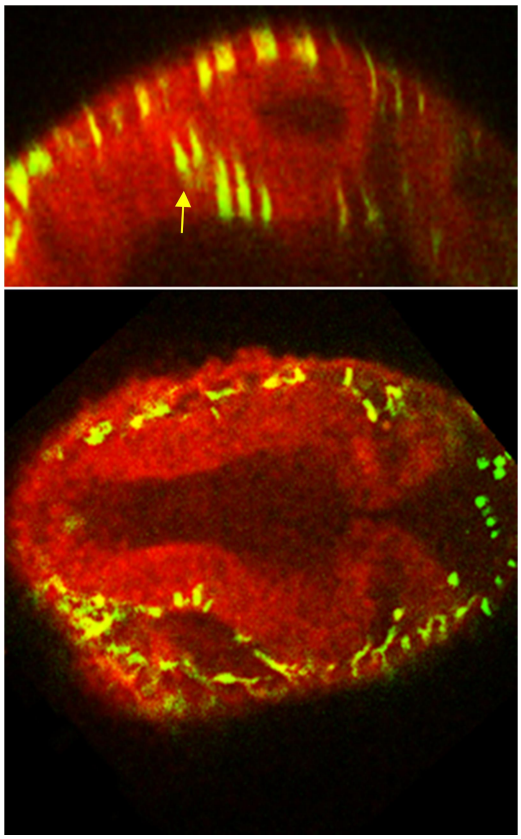

Figure 25: *sox10* reporting 30 hpf.

Perdurance of fluorescence is seen as it appears as there are multiple sets of the triple cell cluster, yet it is only the resilient/residual fluorescence that has a lifetime within the cell after it reports. The cells observed in the lateral slice of the midbrain migrate anteriorly in the neuroepithelium, towards the developing eye. Because there is a large amount of *sox10* expression around the nasal/optic cavity during the development of the embryo, it is hard to distinguish migration in or out of the epithelium in this region. Imaging was conducted out to 40 hpf in this *-4.9eGFP:sox10* line to determine the ultimate fate of this midbrain *sox10* lineage.

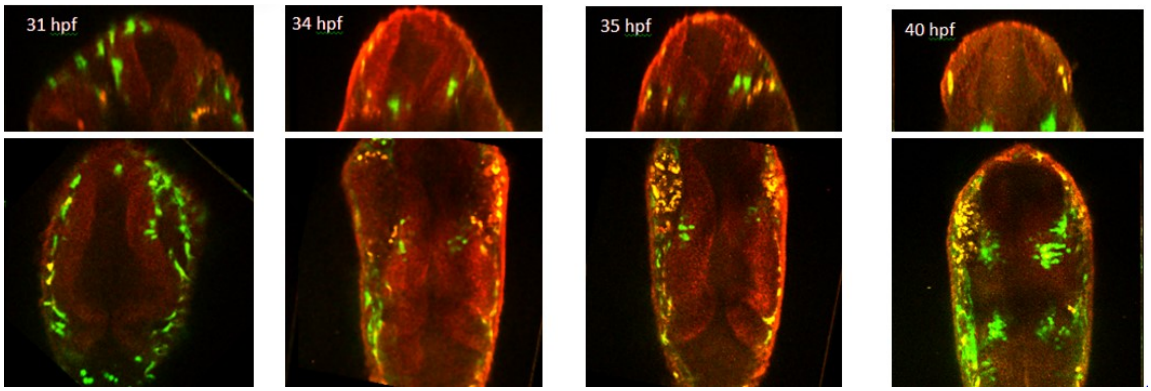

Figure 26: *sox10* reporting 31-40 hpf.

It seems that the general trajectory of these cells towards the nasal/optic cavity or at the very least the frontal portion of the neuroepithelium continues. At the most anterior reaches of the epithelium this *sox10* reporting seems to migrate towards the most dorsal points of the neural tissue in the forebrain as shown below.

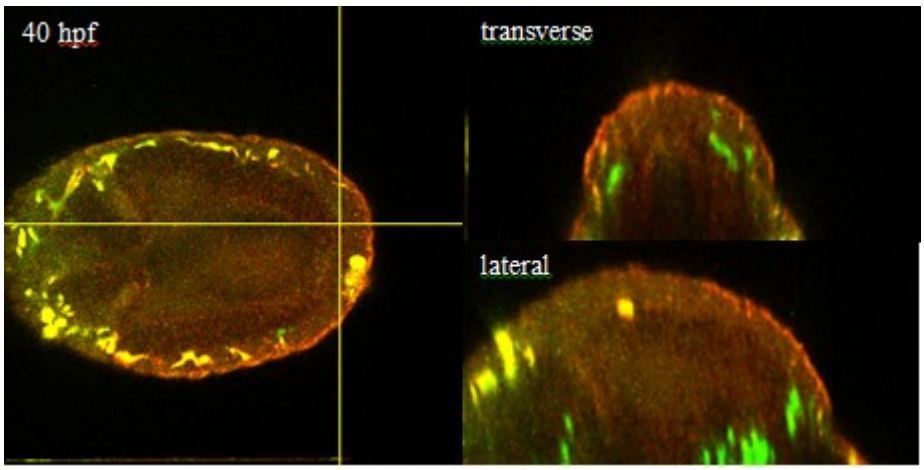

Figure 27: *sox10* reporting 40 hpf.

In the above Figure 27, a transverse slice is taken of the 40 hpf forebrain showing the pervasion of neural crest marking cells in the epithelium. These cells displayed axially in the Figure (26) before are shown to wrap towards this point. Viewing the embryo at the latest timepoint with different aspects of three dimensions is a method of visualizing the extent of proliferation of these cells as shown in Figure 28.

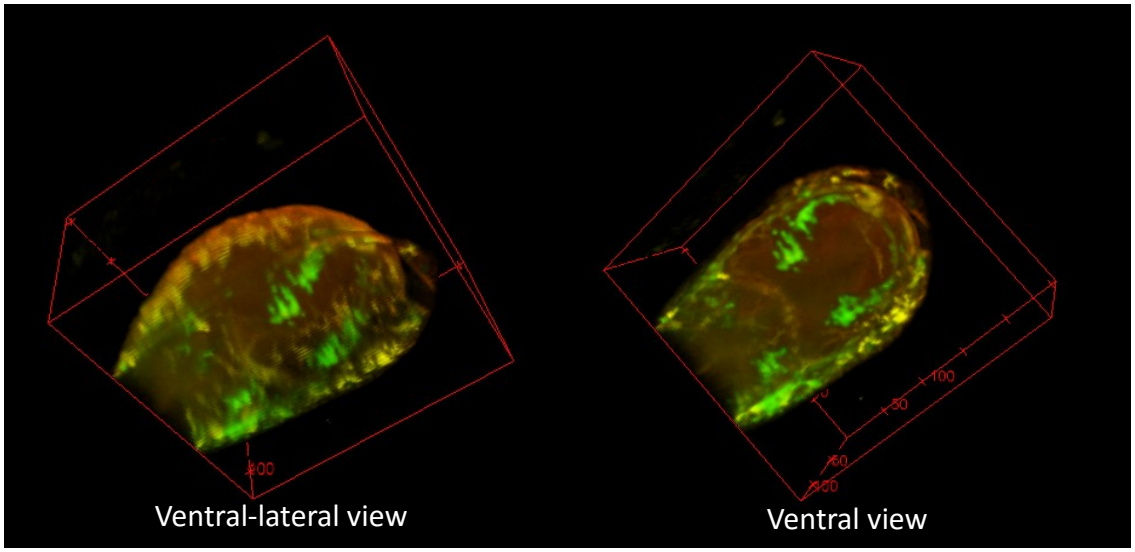

Figure 28: *sox10* reporting in three dimensions.

Narrowing down the list of possible fates for this *sox10* expressing population one would consider many cell types considering the wide variety that neural crest is progenitor to and that *sox10* is related to. Though *sox10* and *mitfa* have well documented relationships, it is possible these cells are related to something other than chromatophore. In zebrafish, *sox10* is not only connected to melanophore pathways but also is associated with glial neural crest progenitors. Glial cells are another subset of neural crest derived cells that aid in composure of the central and peripheral nervous systems. The glial lineage responsible for myelinating axons in the central nervous

system is called oligodendrocyte, while in the peripheral nervous system this is done by Schwann cells. *Olig1*and *Olig2* are transcription factors associated with the progenitors of these oligodendrocyte glial cells and their expression patterns in the diencephalon at 48 hpf coincide with the strong presence of *sox10* expression in this region at 40hpf in Tg(*-4.9sox10:eGFP*). *Sox10* was shown to induce *Olig1*, their concerted activity resulting in myelin expression and deposition (Li, et al. 2007). Perhaps these *sox10* expressing cells are presenting as oligodendrocyte progenitors, or rather inducing their presence. It has been shown that colocalization of *sox10*, *olig1*, and *olig2* indicates midbrain oligodendrocytes reported in the ventral midbrain (Schebesta et al, 2009), and thus experiments to test for colocalization of *Tg(-4.9sox10:eGFP)* reporting and *olig1* expression would confirm that these cells are oligodendrocyte or progenitor to it. In other instances *sox10* reporting has been used to mark oligodendrocytes outright in the midbrain, cytosolic GFP reporting imaged 200 microns from the surface of the optic tectum within matured oligodendrocytes at 72 hpf (Wang et al., 2014). Further evidence suggesting that these cells are involved in the induction of the oligodendrocyte progenitor network are reports that *sox10* knockdown leads to reduced *mbp* (myelin basic protein) in the brain and a total lack of differentiated oligodendrocytes (Carney, 2006).

Sox10 expression has also been reported in the midbrain to play a role in the development of Gonadotropin Releasing Hormone (GnRH) cells in zebrafish. GnRH cells in zebrafish are thought to modulate their reproductive activity. Not only has *sox10*

expression been shown to colocalize with these GnRH cells in pharyngula stages, but these GnRH cells are reduced by downregulation of *sox10* (Whitlock et al., 2005).

Time Lapse Live Imaging of mitfa:eGFP-w47 Line

Similar experiments were conducted to see if melanophore identity gene expression coincided with either the autofluorescence signal or neural crest markers. All *mitfa* expression in the midbrain region was confined to cells that had delaminated from the neuroepithelium and began to dorsolaterally migrate to their fated destinations. This

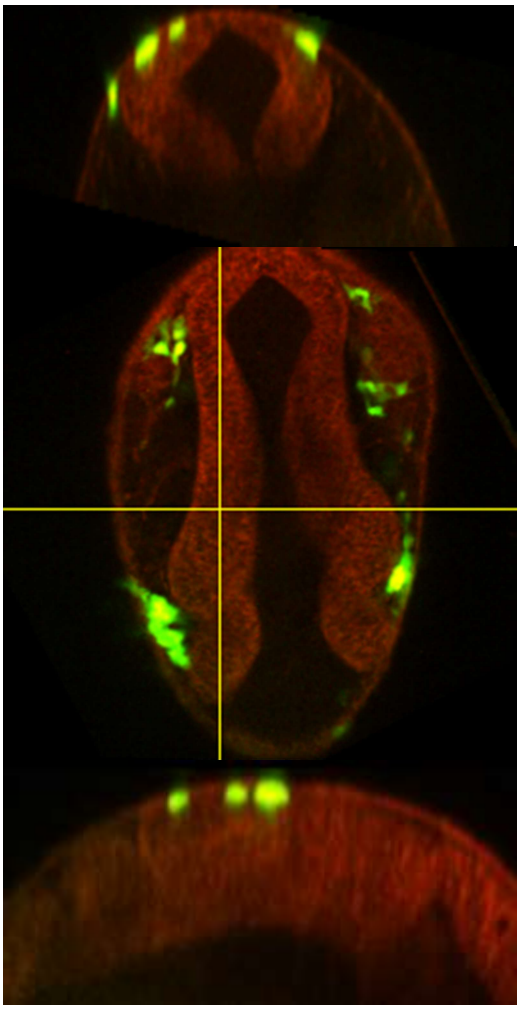

Figure 29: *mitfa* reporting.

timepoint in Figure 29 is representative of most timepoints between 24-28 hpf. There is no significant difference between each time point. This stack is representative of all timepoints of interest, as the only difference between them is the location of the dorsolateral migrating cells post delamination, for this region of interest. However, in the hindbrain neuroepithelium, there are cells within the neuroepithelium presenting *mitfa* expression.

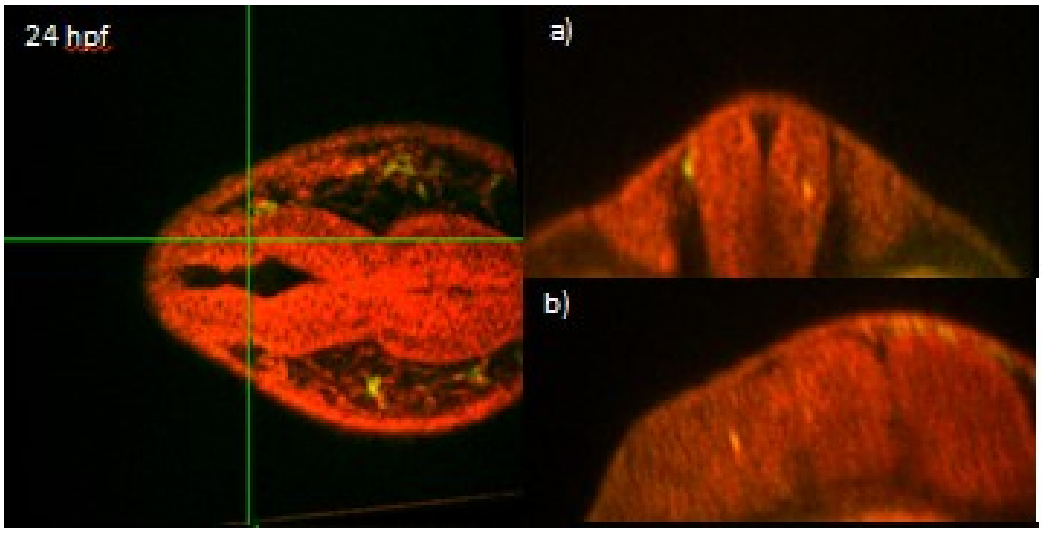

Figure 30: *mitfa* reporting at 24 hpf.

In Figures 30-31 it can be seen that there are small signals developing at prim-5 within the neuroepithelium, just beyond the midbrain-hindbrain barrier towards the trunk.

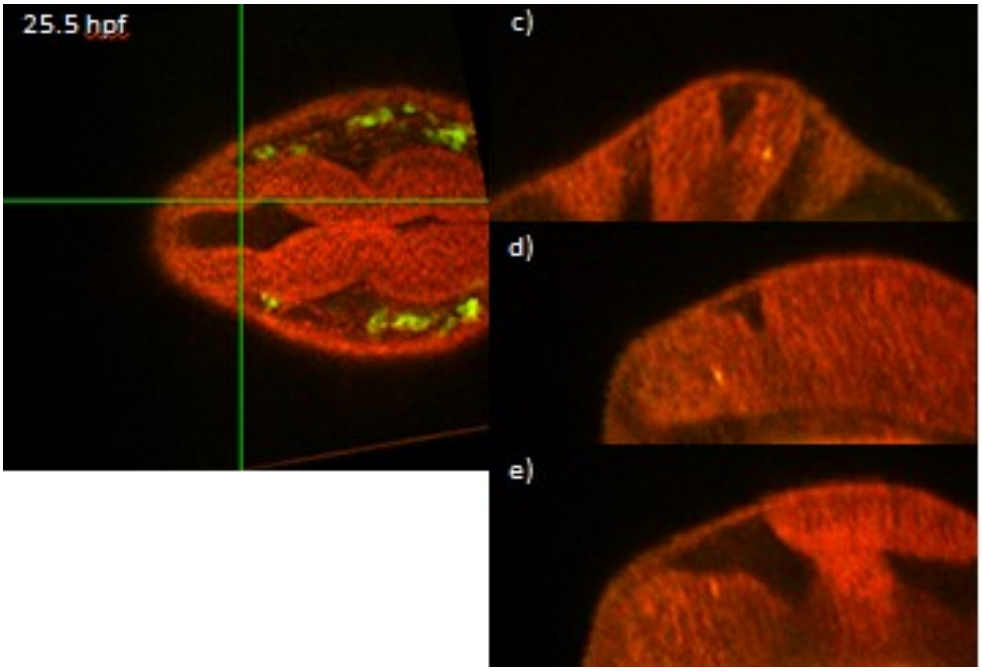

Figure 31: *mitfa* reporting at 25 hpf.

These signals begin to intensify and migrate towards the sagittal plane of the fish, and by 27 hpf (Figure 32) there are several locations in the hindbrain exhibiting small *mitfa* reporting signals.

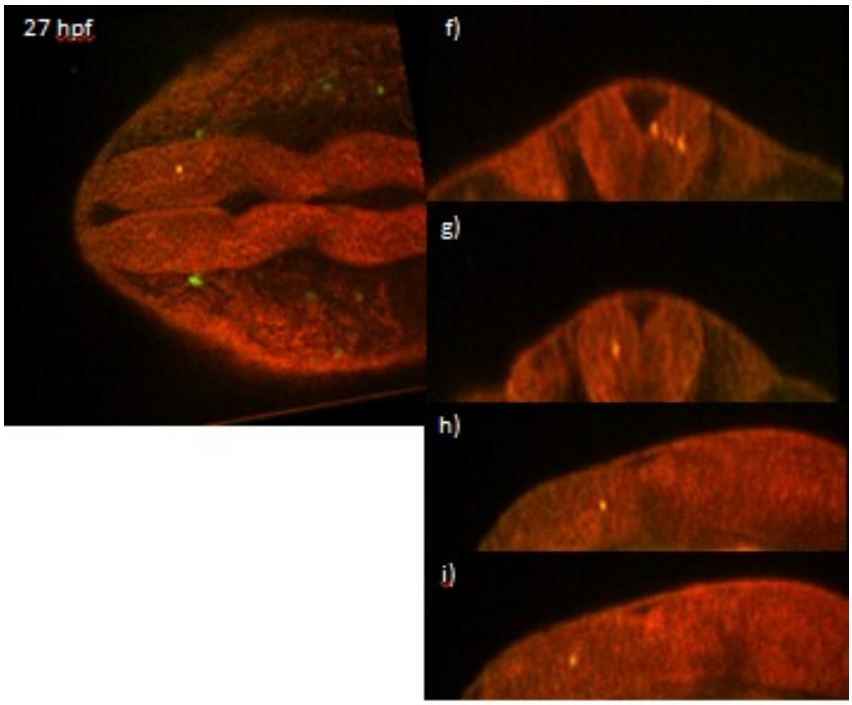

Figure 32: *mitfa* reporting at 27 hpf.

This signal reintroduces the previous idea that differentiation occurs within the neuroepithelium, even well before delamination and that neural crest fate is decided before the transition that is presumed to occur, or alternatively that a subset of melanophores may re-enter the neuroepithelium. Though this is intriguing, the result has no bearing on such a potential behavior in the midbrain. Future characterization and tracking of this population would be interesting, the origin of this particular *mitfa* lineage could be elucidated by more time lapse experiments.

CONCLUDING REMARKS

The studies conducted to reveal the identity of MFCs presented in this report used imaging of reporter fluorescence in time and space to assign genetic identity to cell populations by association with the neural crest marker *sox10* and the melanocyte identity regulator *mitfa*. We observed *sox10* in the neuroepithelium, which raises legitimate questions about the neural crest induction, differentiation, and migration model. This population of cells could be considered to be a unique division of the neural crest or otherwise suggests an unclarified role for *sox10* expression in this region of the brain. Because their ultimate destination is unknown, and can only be speculated as nasal or optical at this point, further scrutiny of this midbrain population could be achieved through more time lapse information, especially 36 hpf and beyond, perhaps as far as 48 hpf when *sox10* expression begins to subside (Greenhill et al., 2011). This imaging is necessary due to the fact that in all timelapse data taken thus far the *sox10* expressing cells are still neuroepithelium bound, thus destination can only be predicted by their trajectory as shown in these time lapse studies. This study suggests that neural crest cells can both begin to differentiate and delaminate from the classical dorsal most point of the neural tube and perhaps from within the epithelium, dwelling and differentiating within the brain. If this population is not marking neural crest, which is possible considering their behavior, then this study portrays another function of *sox10* gene expression besides marking neural crest for this transcription factor. These cells could be linked to glial lineages or another chromatophore, however melanocytes do not seem likely considering the data found in this study.

Time lapse imaging of the Tg(*mitfa:eGFP-w47*) line showed no coincidence of melanophore identity within the midbrain neuroepithelium, at least for timepoints of particular interest in investigation of the autofluorescence signal observed. Hindbrain melanophore identity was observed, however beyond the MHB region of the zebrafish where it was indicated that melanophores can differentiate within the neuroepithelium though they may accumulate directly outside it. Further tracking of these cells would prove interesting to characterize their destination and whether or not they are indeed pigment fated cells of the neural crest.

More is discovered about the gene regulatory networks that govern vertebrate development all the time, and ultrashort pulse microscopy has proven to be a useful method for attaining the spatio-temporal dynamics necessary to clarify these models. In regards to this study, a novel population of cells within the neural crest lineage *sox10* has been demonstrated to reside within the brain of the model organism *Danio rerio* with the technological innovations of ultrashort pulse microscopy

Future Work

Aside from more lime lapse imaging of the reporter for *sox10,* it must be verified that the transcription of *sox10* is active for this reporting data, which can be done via in-situ hybridization experiments. Also, more crest markers should be imaged in this region, such as snail1, *slug/snail2*, *sox8, sox9, foxd3, ap-2,* and *twist* (Klymkowsky et al., 2010). A thorough spatio-temporal model of the crest markers in this region has yet to be achieved due to the lack of feasible method to systematically image crest reporters in four dimensions within the cranial region of zebrafish. Neural plate specifiers and

neural crest markers expression should be better mapped in time and space to clarify their roles in crest induction. UPM could be used to accomplish the mapping of the gene regulatory network in this cranial region, especially pertaining to the cranial neural crest with excellent temporal resolution. This can be accomplished using more transgenic lines to study the crest and the effector genes that aid in fate specification, via time lapse imaging experiments. To thoroughly investigate the epithelium bound *sox10* expressing population observed in this study, these other transgenic reporters would need to be studied to clarify their presence. *Twist* plays a large role in cranial neural crest migration, whereas *slug* is thought to mediate epithelial dissociation (Gilbert 2010). Because the aforementioned population of *sox10* expressing cells does not seem to dissociate from the epithelium or migrate to a destination (at least within the window observed) it would be valuable to study expression of *twist* and *slug* genes in this region, or a lack thereof. It is not certain that these *sox10* expressing cells did not delaminate from another region of the neural tissue as classic theory would require, as they may have delaminated near the hindbrain and taken a medial pathway towards the midbrain, and then re-entered the tissue it had just removed itself from. Increasing the temporal resolution during neural crest marker reporting experiments could aid in capturing such a migratory event.

Further imaging experiments could clarify a potential role of these cells in oligodendrocyte induction. It has been reported that there are oligodendrocytes marked by *sox10* in this region of the diencephalon by 72 hpf (Wang et al., 2014), and the data produced in this study could represent the early expression and induction of this population. A straightforward test of this hypothesis would be to image these Tg(-

4.9sox10:eGFP) fish live from 40-48 hpf when *olig1* expression is expected to begin, followed by fixation. After imaging GFP reporting, the fish would undergo an ISH for *olig1* and these image sets could be registered to display colocalization. Similar experiments could be conducted at earlier time points to determine whether coincidence of expression occurs earlier. Additionally, ISH is needed to verify that eGFP reporting for *sox10* is indicative of active transcription at each of these timepoints, as GFP perdurance can last upwards of twelve hours. Due to the possibility that there is *sox10* utility within the midbrain for both glial cells and another subset of cells, the midbrain GnRH population, it is necessary to clarify which cells within the midbrain are engaged in which gene regulatory network. Reporting of *GnRH* in relation to *sox10* and *olig1* transcription factors could highlight co-involvement or separation of patterning in these potentially multipotent neural crest derived midbrain cells. These experiments could potentially clarify the role of this novel neural crest population and clarify neural crest/glial cell induction gene regulatory networks. Furthermore, if this population is implicated as glial progenitor, future studies detailing results of manipulation of these transcription factors in relation to *mbp* in the brain could clarify mechanisms of demyelinating diseases in vertebrates. WT embryo fixation experiments should be conducted with fixatives without aldehydes to determine conclusively that aldehydes are the cause of the alleged MFC signal observed prior, though the live imaging studies presented within this work were quite conclusive.

REFERENCES

Band, Yehuda Benzion. Light and Matter: Electromagnetism, Optics, Spectroscopy and Lasers. Chichester: John Wiley, 2006.

Beyersdorf, Peter. "Short Pulse Generation." Review. Audio blog post. Laser Spectroscopy Podcast. N.p., 16 Nov. 2009.

Butler, Ann B., and William Hodos. Comparative Vertebrate Neuroanatomy: Evolution and Adaptation. New York: Wiley-Liss, 1996.

Carney, T. J., K. A. Dutton, E. Greenhill, M. Delfino-Machin, P. Dufourcq, P. Blader, and R. N. Kelsh. "A Direct Role for Sox10 in Specification of Neural Crest-derived Sensory Neurons." Development 133.23 (2006): 4619-630.

Chen, Xiyi, Oleg Nadiarynkh, Sergey Plotnikov, and Paul J. Campagnola. "Second Harmonic Generation Microscopy for Quantitative Analysis of Collagen Fibrillar Structure." Nat Protoc Nature Protocols 7.4 (2012): 654-69.

Cinelli, Riccardo A. G., Aldo Ferrari, Vittorio Pellegrini, Mudit Tyagi, Mauro Giacca, and Fabio Beltram. "The Enhanced Green Fluorescent Protein as a Tool for the Analysis of Protein Dynamics and Localization: Local Fluorescence Study at the Single-molecule Level." Photochemistry and Photobiology 71.6 (2000): 771-76.

Cox, Guy, Eleanor Kable, Allan Jones, Ian Fraser, Frank Manconi, and Mark D. Gorrell. "3-Dimensional Imaging of Collagen Using Second Harmonic Generation." Journal of Structural Biology 141.1 (2003): 53-62.

Curran, Kevin, James A. Lister, Gary R. Kunkel, Andrew Prendergast, David M. Parichy, and David W. Raible. "Interplay between Foxd3 and Mitf Regulates Cell Fate Plasticity in the Zebrafish Neural Crest."Developmental Biology 344.1 (2010): 107-18.

Davenport, D. & J.A.C. Nicol. Luminescence in Hydromedusae. Proc. R. Soc. London Ser. B 144: 399–411(1955).

Drobizhev, Mikhail, Nikolay S. Makarov, Shane E. Tillo, Thomas E. Hughes, and Aleksander Rebane. "Two-photon Absorption Properties of Fluorescent Proteins." Nature Methods Nat Meth 8.5 (2011): 393-99.

Dutton, James R., Anthony Antonellis, Thomas J. Carney, Frederico Slm Rodrigues, William J. Pavan, Andrew Ward, and Robert N. Kelsh. "An Evolutionarily Conserved Intronic Region Controls the Spatiotemporal Expression of the Transcription Factor Sox10." BMC Developmental Biology BMC Dev Biol 8.1 (2008): 105.

Elsalini OA and Rohr KB. Dev Genes Evol. 212(12):593-598. (2003).

Geldmacher-Voss, B., Reugels, A.M., Pauls, S., Campos-Ortega, J.A.A 90 degrees rotation of the mitotic spindle changes the orientation of mitoses of zebrafish neuroepithelial cells. Development. 130, 3767–3780 (2003).

Gibbs, Holly C., Yuqiang Bai, Arne C. Lekven, and Alvin T. Yeh. "Imaging Embryonic Development with Ultrashort Pulse Microscopy." Optical Engineering 53.5: 051506 (2014).

Gibbs, Holly C., Colin R. Dodson, Yuqiang Bai, Arne C. Lekven, and Alvin T. Yeh. "Combined Lineage Mapping and Gene Expression Profiling of Embryonic Brain Patterning Using Ultrashort Pulse Microscopy and Image Registration." J. Biomed. Opt Journal of Biomedical Optics 19.12 (2014): 126016.

Gilbert, Scott F. Developmental Biology. Sunderland, MA: Sinauer Associates (2010).

Goyal, V. "Lipofuscin Pigment Accumulation in Human Brain during Aging."Experimental Gerontology 17.6 (1982): 481-87.

Greenhill, Emma R., Andrea Rocco, Laura Vibert, Masataka Nikaido, and Robert N. Kelsh. "An Iterative Genetic and Dynamical Modelling Approach Identifies Novel Features of the Gene Regulatory Network Underlying Melanocyte Development." PLoS Genetics PLoS Genet 7.9 (2011).

Hall, Andrea M., and Seth J. Orlow. "Degradation of Tyrosinase Induced by Phenylthiourea Occurs following Golgi Maturation." Pigment Cell Research 18.2: 122-29 (2005).

Hassel, J. and Hand, A.R. J. Histochem. Cytochem. 22 229-239 (1974).

Helmchen, Fritjof, and Winfried Denk. "Deep Tissue Two-photon Microscopy." Nature Methods Nat Meth 2.12 (2005): 932-40.

Karlsson, Johnny, Jonas Von Hofsten, and Per-Erik Olsson"Generating Transparent Zebrafish: A Refined Method to Improve Detection of Gene Expression During Embryonic Development." Marine Biotechnology 3.6: 0522-527 (2001).

Kiernan, John. Autofluorescence: Causes and CuresTable of Contents (n.d.): n. pag.Toronto Western Research Institute, University Health Network. Wright Cell Imaging Facility. 2004.

Kishi, Shuji, Junzo Uchiyama, Anne M. Baughman, Tadateru Goto, Mao C. Lin, and Stephanie B. Tsai. "The Zebrafish as a Vertebrate Model of Functional Aging and Very Gradual Senescence." Experimental Gerontology 38.7 (2003): 777-86.

Kremers, Gert-Jan, Sarah G. Gilbert, Paula J. Cranfill, Michael W. Davidson, and David W. Piston. "Fluorescent Proteins at a Glance." Journal of Cell Science. Company of Biologists, 2016.

Krispin, Shlomo, Erez Nitzan, and Chaya Kalcheim. "The Dorsal Neural Tube: A Dynamic Setting for Cell Fate Decisions." Developmental Neurobiology 70.12 (): 796-812 (2010).

Klymkowsky, Michael W., Christy Cortez Rossi, and Kristin Bruk Artinger. "Mechanisms Driving Neural Crest Induction and Migration in the Zebrafish and Xenopus Laevis." Cell Adhesion & Migration. Landes Bioscience, 2010.

Lacosta, Ana M., Jesus Canudas, Cristina Gonzalez, Pedro Muniesa, Manuel Sarasa, and Luis Dominguez. "Pax7 Identifies Neural Crest, Chromatophore Lineages and Pigment

Stem Cells during Zebrafish Development." Int. J. Dev. Biol. The International Journal of Developmental Biology 51.4 (2007): 327-31.

Li, H., Y. Lu, H. K. Smith, and W. D. Richardson. "Olig1 and Sox10 Interact Synergistically to Drive Myelin Basic Protein Transcription in Oligodendrocytes." Journal of Neuroscience 27.52 (2007): 14375-4382.

Long, Q., A. Meng, H. Wang, J.R. Jessen, M.J. Farrell & S. Lin. GATA-1 expression pattern can be recapitulated in living transgenic zebrafish using GFP reporter gene. Development 124: 4105–4111 (1997).

M. Westerfield, The zebrafish book. A guide for the laboratory use of zebrafish (Danio rerio). 4th ed., Univ. of Oregon Press, Eugene (2000).

Meulemans D, Bronner-Fraser M. Gene-regulatory interactions in neural crest evolution and development. Dev Cell 2004; 7:291-9.

Mort, Richard L., Jackson Ian, and Elizabeth E. Patton. "The Melanocyte Lineage in Development and Disease." Development: The Company of Biologists, 2015.

Nakamura, Harukazu. "Regionalization of the Optic Tectum: Combinations of Gene Expression That Define the Tectum." Trends in Neurosciences24.1 (2001): 32-39.

Schebesta, M., and Serluca, F.C. olig1 expression identifies developing oligodendrocytes in zebrafish and requires hedgehog and notch signaling. Dev. Dyn. 238(4): 887-898. (2009)

Shen, Y. R. The Principles of Nonlinear Optics. New York: J. Wiley, 1984.

So, Peter Tc. "Two-photon Fluorescence Light Microscopy." ELS (2001)

Svelto, Orazio. Principles of Lasers. New York: Springer, 2005.

Svoboda, Karel, and Ryohei Yasuda. "Principles of Two-Photon Excitation Microscopy and Its Applications to Neuroscience." Neuron 50.6 (2006): 823-39.

Wang, K. et al. Nat. Methods 11, 625–628 (2014).

Whitlock, K. E. "A Role for Foxd3 and Sox10 in the Differentiation of Gonadotropin-releasing Hormone (GnRH) Cells in the Zebrafish Danio Rerio." Development 132.24 (2005): 5491-502.

Wu, Qiaofeng, Brian E. Applegate, and Alvin T. Yeh. "Cornea Microstructure and Mechanical Responses Measured with Nonlinear Optical and Optical Coherence Microscopy Using Sub-10-fs Pulses."Biomed. Opt. Express Biomedical Optics Express 2.5:1135. (2011)

Yeh, Alvin T., Holly Gibbs, Jin-Jia Hu, and Adam M. Larson. "Advances in Nonlinear Optical Microscopy for Visualizing Dynamic Tissue Properties in Culture." Tissue Engineering Part B: Reviews 14.1: 119-31.(2008)

Zipfel, W. R., R. M. Williams, R. Christie, A. Y. Nikitin, B. T. Hyman, and W. W. Webb. "Live Tissue Intrinsic Emission Microscopy Using Multiphoton-excited Native Fluorescence and Second Harmonic Generation."Proceedings of the National Academy of Sciences 100.12 (2003): 7075-080.